



Article

# Dynamical Properties of a Stochastic Tumor–Immune System with Impulsive Perturbations and Regime Switching

Junfeng Zhao <sup>1</sup>, Bingshuo Wang <sup>2</sup>, Wei Li <sup>2</sup>,\*, Dongmei Huang <sup>2</sup> and Vesna Rajic <sup>3</sup>

- School of Mathematics and Statistics, Northwestern Polytechnical University, Xi'an 710071, China; zhaojf@nwpu.edu.cn (J.Z.)
- School of Mathematics and Statistics, Xidian University, Xi'an 710071, China; 22071213269@stu.xidian.edu.cn (B.W.); dmhuang@xidian.edu.cn (D.H.)
- Department for Statistics and Mathematics, Faculty of Economics and Business, University of Belgrade, 11000 Belgrade, Serbia; vesna.rajic@ekof.bg.ac.rs
- \* Correspondence: liweilw@mail.xidian.edu.cn

Abstract: Despite numerous clinical attempts to treat tumors, malignant tumors remain a significant threat to human health due to associated side effects. Consequently, researchers are dedicated to studying the dynamical evolution of tumors in order to provide guidance for therapeutic treatment. This paper presents a stochastic tumor-immune model to discover the role of the regime switching in microenvironments and analyze tumor evolution under comprehensive pulse effects. By selecting an appropriate Lyapunov function and applying Itô's formula, the ergodicity theory of Markov chains, and inequality analysis methods, we undertake a systematic investigation of a tumor's behavior, focusing on its extinction, its persistence, and the existence of a stationary distribution. Our detailed analysis uncovers a profound impact of environmental regime switching on the dynamics of tumor cells. Specifically, we find that when the system is subjected to a high-intensity white noise environment over an extended duration, the growth of tumor cells is markedly suppressed. This critical finding reveals the indispensable role of white noise intensity and exposure duration in the long-term evolution of tumors. The tumor cells exhibit a transition from persistence to extinction when the environmental regime switches between two states. Furthermore, the growth factor of the tumor has an essential influence on the steady-state distribution of the tumor evolution. The theoretical foundations in this paper can provide some practical insights to develop more effective tumor treatment strategies, ultimately contributing to advancements in cancer research and care.

**Keywords:** tumor–immune interaction; stochastic perturbations; regime switching; impulsive perturbations; persistence and extinction

MSC: 37A50; 58K30; 65D25; 92-10



Academic Editor: Takashi Suzuki

Received: 24 January 2025 Revised: 3 March 2025 Accepted: 10 March 2025 Published: 11 March 2025

Citation: Zhao, J.; Wang, B.; Li, W.; Huang, D.; Rajic, V. Dynamical Properties of a Stochastic Tumor–Immune System with Impulsive Perturbations and Regime Switching. *Mathematics* **2025**, *13*, 928. https://doi.org/10.3390/ math13060928

Copyright: © 2025 by the authors. Licensee MDPI, Basel, Switzerland. This article is an open access article distributed under the terms and conditions of the Creative Commons Attribution (CC BY) license (https://creativecommons.org/licenses/by/4.0/).

#### 1. Introduction

Cancer is one of the most severe global health threats; its high mortality rate makes effective treatment a critical topic in medical research. Although existing therapies [1–4] such as surgery, radiotherapy, chemotherapy, and immunotherapy have improved patient survival rates to some extent, the complexity of cancer presents multiple challenges for treatment. In particular, the complicated interactions between the immune system and tumors pose a core issue in clinical practice: how to effectively control tumor growth and improve therapeutic outcomes.

Mathematics **2025**, 13, 928

In recent years, comprehensive pulsed therapy has attracted increasing attention as a comprehensive strategy by combining chemotherapy with immunotherapy. This approach utilizes periodic pulsed treatments to reduce side effects and enhance immune responses, thereby improving therapeutic efficiency [5,6]. Under single-mode treatment, chemotherapy or immunotherapy alone often struggles to fully control tumors or may lead to drug resistance or adverse effects. In contrast, combining immunotherapy with chemotherapy can significantly improve therapeutic outcomes and counteract tumor resistance [6]. Some valuable work associated with comprehensive pulsed therapy has shown the advantages of this therapy. For example, ref. [7] constructed a stochastic pulsed dynamical model to study tumor evolution and extinction conditions under combined chemotherapy and immunotherapy. Their results showed that comprehensive treatment profoundly influences tumor progression and, under specific conditions, can lead to complete tumor cell eradication. Moreover, their model indicates that varying doses and intervals of pulsed therapy have an optimal combination for better therapeutic outcomes [8]. In addition, a hybrid treatment model proposed in [9] reveals that low-dose chemotherapy combined with intensive immunotherapy effectively alleviates side effects while enhancing overall treatment efficiency. Thus, by integrating the advantages of chemotherapy and immunotherapy, comprehensive pulsed therapy not only optimizes therapeutic outcomes but also reduces side effects, providing more personalized and effective treatment strategies for cancer patients.

However, most existing studies are limited to deterministic frameworks [10–15], neglecting the impact of environmental fluctuations on treatment efficacy. In reality, factors such as tumor growth rates, immune responses, and other biological parameters are frequently influenced by environmental changes, including variations in drug concentrations and immune activity. Traditional deterministic models are inadequate in capturing such uncertainties. In tumor-immune modeling, stochasticity has proven to significantly influence system dynamics: different types of stochastic noise, such as Lévy noise and Gaussian white noise, can induce state transitions in tumors [16]; the correlation strength of noise directly determines stability and transition probabilities during treatment [17]; and stochastic resonance phenomena highlight the potential for synergistic optimization between noise and therapeutic parameters, significantly enhancing treatment outcomes [18]. Additionally, noise impacts the steady-state distribution and statistical properties of the system, providing critical guidance for treatment strategy design [19]. These findings collectively validate the central role of stochasticity in dynamic tumor modeling and therapy optimization. Therefore, incorporating stochasticity into tumor–immune models is essential to improve model precision and real-world applicability.

Furthermore, as the understanding of tumor–immune mechanisms has deepened, an increasing number of studies have introduced stochastic switching mechanisms to simulate the dynamic changes in tumor growth and immune response processes. By employing Markov chains to characterize stochastic switching, it is possible to effectively capture system parameter fluctuations induced by environmental changes, offering more precise and detailed mathematical descriptions for cancer treatment. Ref. [20] constructed a stochastic tumor–immune model with pulse treatment and demonstrated the impact of stochastic and pulsed disturbances on tumor cell extinction dynamics, emphasizing the critical role of environmental randomness in treatment outcomes. Ref. [21] proposed a tumor–immune model regulated by a Markov chain, deriving threshold conditions to reveal how environmental parameter changes determine tumor cell extinction or long-term survival. Moreover, ref. [22] explored a prostate cancer model incorporating Gaussian white noise and environmental switching, finding that the combined effects of high-intensity noise and environmental switching effectively suppressed tumor development and improved patient quality of life. These studies indicate that stochastic switching and environmental

Mathematics 2025, 13, 928 3 of 29

fluctuations are crucial factors for optimizing tumor immunotherapy strategies, providing theoretical support for more precise treatment protocols.

During specific antitumor immune responses, helper T-cells and hunting T-cells form functionally complementary dual-track mechanisms: Helper T-cells are activated by recognizing MHC class II molecular complexes on antigen-presenting cells (e.g., macrophages), subsequently secreting cytokines such as IL-2 and transmitting co-stimulatory signals to establish the essential microenvironment for hunting T-cell proliferation and differentiation [23]. Upon activation, hunting T-cells rely on MHC class I molecules to precisely identify tumor-specific antigen epitopes, triggering target cell apoptosis via perforin-granzyme complex release, while simultaneously generating immunological memory to prevent recurrence [24,25]. These two subsets synergize through hierarchical antigen presentation and coordinated signaling cascades, constructing a spatiotemporally dynamic immune clearance network against malignant cells. Nevertheless, studies such as [20,21] only consider two populations—tumor cells or tumor cells with hunting T-cells—while ignoring the presence of helper T-cells. Although [26] accounted for three cell types, it did not consider stochastic switching. Therefore, this study proposes a new stochastic switching model based on three populations: tumor cells, hunting T-cells, and helper T-cells. By incorporating pulse therapy and stochastic switching, this model aims to explore the effects of environmental fluctuations on tumor immunotherapy and provide optimized strategies and theoretical support for cancer treatment.

# 2. Tumor-Immune Model and Preliminaries

## 2.1. Stochastic Tumor–Immune Model with Pulsed Effect and Regime Switching

In research on tumor immunodynamics, Kaur [27] employed a Michaelis–Menten kinetic model to elucidate cytokine-mediated dynamic interactions between helper T-cells and tumor cells, demonstrating that the biological threshold of affinity enhancement effectively suppresses tumor proliferation. Based on this framework, Wang [28] introduced stochastic perturbations through Gaussian white noise to quantify microenvironmental fluctuations while delineating the tripartite regulatory network involving tumor cells, hunting T-cells, and helper T-cells (Figure 1). Subsequently, Li [29] advanced this paradigm by establishing the following integrated stochastic immune–oncology model that incorporates both biological noise and periodic variations due to pharmacological interventions:

$$\begin{cases}
dT(t) = \left(a_{1}T\left(1 - \frac{T}{c_{1}}\right) - b_{1}TH\right)dt + \sigma_{1}TdB_{1}(t), \\
dH(t) = (\gamma HR - d_{1}H - b_{2}HT)dt + \sigma_{2}HdB_{2}(t), \\
dR(t) = \left(a_{2}R\left(1 - \frac{R}{c_{2}}\right) - \gamma HR - d_{2}R + \frac{hTR}{T+g}\right)dt + \sigma_{3}RdB_{3}(t),
\end{cases} t \neq nP, n \in Z^{+},$$

$$T(nP^{+}) = [1 - \alpha(nP)]T(nP), \\
H(nP^{+}) = [1 + \beta(nP)]H(nP), \\
R(nP^{+}) = R(nP),
\end{cases} t = nP, n \in Z^{+},$$
(1)

where T(t), H(t), and R(t) represent the populations of tumor cells, hunting T-cells, and helper T-cells, respectively. The initial conditions of the model are T(0) > 0, H(0) > 0, and R(0) > 0. The parameters include the intrinsic growth rates of tumor cells and helper T-cells, denoted as  $a_i$  (i = 1, 2), and the environmental carrying capacities, denoted as  $c_i$  (i = 1, 2). The interaction between tumor cells and hunting T-cells leads to the loss rate  $b_i$  (i = 1, 2), while the death rates of hunting T-cells and helper T-cells are given by  $d_i$  (i = 1, 2). Additionally, helper T-cells activate hunting T-cells at a rate of  $\gamma$ , and their proliferation occurs at the rate h with the half-saturation constant g. The terms  $B_i(t)$  (i = 1, 2, 3) represent independent Brownian motions, and  $\sigma_i$  (i = 1, 2, 3) denote their

Mathematics **2025**, 13, 928 4 of 29

corresponding noise intensities. The parameter P denotes the time interval between two consecutive pulse therapies. The function a(nP) represents the tumor cell killing rate during the n-th chemotherapy cycle, while b(nP) denotes the recruitment rate of hunting T-cells during the n-th immunotherapy cycle.

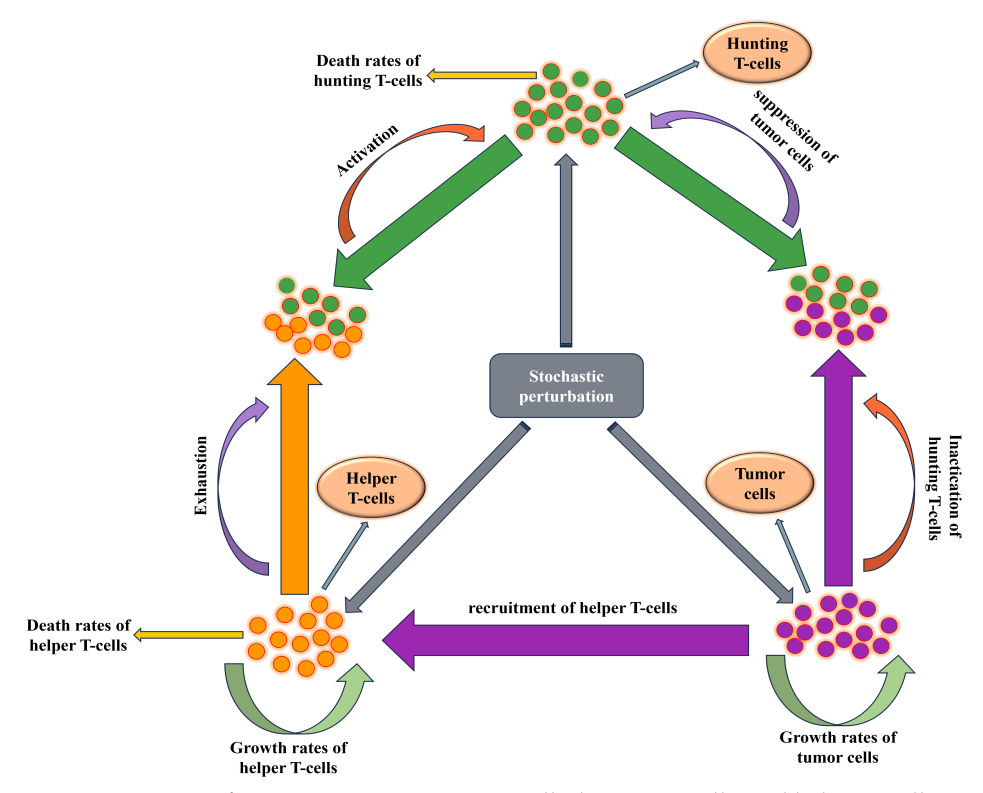


Figure 1. Diagram of interactions among tumor cells, hunting T-cells, and helper T-cells.

Markov chains demonstrate unique advantages in modeling environmental stochasticity within complex biological systems: First, their finite-state switching mechanism [22,30] effectively captures discontinuous transitions in tumor microenvironments or host immune states, utilizing steady-state distributions to quantify the regulatory effects of multi-state residence probabilities on system dynamics. Second, coupling Markov chains with white noise [20,31] enables the differentiation of temporal-scale environmental perturbations; the state transitions (colored noise) drive macroscopic behavioral evolution (e.g., tumor drug-resistant phenotypic switching), while white noise captures transient parameter fluctuations (e.g., random variations in drug metabolic rates). These properties solidify Markov chains as an ideal framework for integrating environmental heterogeneity, therapeutic perturbations, and biological adaptive mechanisms. To better capture the dynamic changes in the external environment and their impact on the tumor-immune system, this study incorporates a continuous-time finite-state Markov chain into the model. The interactions among tumor cells, hunting T-cells, and helper T-cells after incorporating the Markov chain are shown in Figure 1. The rationale for this approach lies in the observation that variations in external conditions can lead to abrupt changes in tumor growth rates, immune response intensity, and other biological parameters. For instance, paclitaxel effectively suppresses tumor growth at a dosage of 28 mg/kg but becomes almost ineffective at 10 mg/kg [26]. Such abrupt changes cannot be adequately characterized by traditional Gaussian white noise. By modeling these variations as state transitions governed by a Markov chain, it becomes possible to represent the system's behavior under distinct environmental states and provide a more comprehensive understanding of tumor-immune dynamics under complex environmental conditions. Based on this refinement, the original system model is modified as follows:

Mathematics 2025, 13, 928 5 of 29

$$\begin{cases} dT(t) = \left(a_{1}(r(t))T\left(1 - \frac{T}{c_{1}(r(t))}\right) - b_{1}(r(t))TH\right)dt + \sigma_{1}(r(t))TdB_{1}(t), \\ dH(t) = (\gamma(r(t))HR - d_{1}(r(t))H - b_{2}(r(t))HT)dt + \sigma_{2}(r(t))HdB_{2}(t), \\ dR(t) = \left(a_{2}(r(t))R\left(1 - \frac{R}{c_{2}(r(t))}\right) - \gamma(r(t))HR - d_{2}(r(t))R + \frac{h(r(t))TR}{T + g(r(t))}\right)dt + \sigma_{3}(r(t))RdB_{3}(t), \end{cases} \end{cases} t \neq nP, n \in Z^{+},$$

$$T(nP^{+}) = [1 - \alpha(nP)]T(nP),$$

$$H(nP^{+}) = [1 + \beta(nP)]H(nP),$$

$$R(nP^{+}) = R(nP), \end{cases} t = nP, n \in Z^{+}.$$

$$(2)$$

In which r(t) denotes a continuous-time finite-state Markov chain with the state space  $\mathcal{M} = \{1, 2, \dots, m\}$ , characterizing the stochastic dynamics of environmental changes. The parameters  $a_i(r(t)), b_i(r(t)), c_i(r(t)), d_i(r(t))$  (i = 1, 2),  $\gamma(r(t)), h(r(t))$ , and g(r(t)) are statedependent functions governed by the current state of r(t). The inclusion of r(t) enables the model to capture sudden shifts in biological and environmental conditions, enhancing its ability to reflect the realistic dynamics of the tumor-immune system under variable external influences.

#### 2.2. Preliminaries

Let  $\{r(t), t \ge 0\}$  be a right-continuous Markov chain [31] defined in the complete filtered probability space  $(\Omega, \mathcal{F}, \{\mathcal{F}_t\}_{t\geq 0}, P)$ , with the finite state space  $\mathcal{M} = \{1, 2, \dots, m\}$ . The transitions are governed by the generator matrix  $\Xi = (\theta_{ij})_{m \times m'}$  defined as

$$P\{r(t+\Delta) = j | r(t) = i\} = \begin{cases} \theta_{ij}\Delta + o(\Delta), & i \neq j, \\ 1 + \theta_{ii}\Delta + o(\Delta), & i = j. \end{cases}$$

Where  $\theta_{ij} \geq 0$  denotes the transition rate from the state *i* to the state *j*. For  $i \neq j$ , it holds that  $\theta_{ii} = -\sum_{i \neq i} \theta_{ii}$ . Under the assumption that  $\theta_{ij} > 0$ , the Markov chain is irreducible and independent of the Brownian motion  $B(\cdot)$ . Consequently, the Markov chain admits the unique stationary distribution  $\pi = (\pi_1, \dots, \pi_m) \in \mathbb{R}^{1 \times m}$ , determined by solving

$$\pi\Xi = 0, \quad \sum_{k=1}^{m} \pi_k = 1.$$

**Definition 1** ([32]).  $X(t) = (T(t), H(t), R(t))^T$ , where  $t \in R_+$ , is called the solution to the ISDE Differential system if (Impulse Stochastic Equation) the following conditions:

- X(t) is absolutely continuous in the intervals (0, P] and (nP, (n+1)P],  $n \in Z^+$ ; (1)
- For each nP,  $n \in \mathbb{Z}^+$ , we have

$$X(nP^{-}) = \lim_{t \to nP^{-}} X(t), \quad X(nP^{+}) = \lim_{t \to nP^{+}} X(t), \quad and \quad X(nP) = X(nP^{-});$$

X(t) satisfies the given system equation for  $t \in \mathbb{R}^+ \setminus \{nP, n \in \mathbb{Z}^+\}$ , and at each  $t = nP, n \in \mathbb{Z}^+$  $Z^+$ , it satisfies the impulse condition.

**Definition 2** ([32]). For any solution  $X(t) = (x_1(t), x_2(t), x_3(t))$  of the system, the following hold:

- If  $\lim_{t\to +\infty} x_i(t) = 0$ , i = 1, 2, 3, then  $x_i(t)$  is said to be extinct;
- (2) If  $\lim_{t\to\infty}\frac{1}{t}\int_0^t x_i(s)\,ds=0$ , i=1,2,3, then  $x_i(t)$  is said to be non-persistent in the mean; (3) If  $\lim_{t\to\infty}\frac{1}{t}\int_0^t x_i(s)\,ds>0$ , i=1,2,3, then  $x_i(t)$  is said to be weakly persistent.

Mathematics 2025, 13, 928 6 of 29

**Lemma 1** ([33]). Suppose  $G(t) \in C(\Omega \times R_+, R_+ \setminus \{0\})$ . If there exist the positive constants  $\lambda_0$ , T, and  $\lambda \geq 0$ , such that for all  $t \geq T$ , G(t) satisfies the inequality

$$\ln G(t) \leq (or \geq) \lambda t - \lambda_0 \int_0^t G(s) \, ds + \sum_{i=1}^n \beta_i B_i(t),$$

where  $\beta_i$   $(1 \le i \le n)$  are constants, then  $\overline{G(t)^*} \le (or \ge) \frac{\lambda}{\lambda_0}$ .

Lemma 2 ([34]). Assume that the following conditions hold:

- (1) For any  $i \neq j$ , it holds that  $\theta_{ij} > 0$ .
- (2) For each  $k \in \mathcal{M}$ , the diffusion matrix D(X,k) is symmetric and satisfies the inequality

$$\rho |\zeta|^2 \le \zeta^\top D(X, k)\zeta \le \frac{1}{\rho} |\zeta|^2, \quad \forall \zeta \in \mathbb{R}^n,$$

where  $\rho \in (0,1]$  is a constant independent of  $X \in \mathbb{R}^n$ .

(3) There exists a bounded, open subset,  $D \subset R^n$ , with a smooth boundary such that, for each  $k \in \mathcal{M}$ , there exists a nonnegative function  $V(\cdot, k) : D^C \to R$ . The function  $V(\cdot, k)$  is twice continuously differentiable in  $D^C$  and satisfies

$$LV(X,k) \leq -\xi$$
,

for some constant,  $\xi > 0$ , and all  $(X, k) \in D^{\mathbb{C}} \times \mathcal{M}$ .

Under these conditions, the system is ergodic and positive recurrent. Specifically, there exists a unique stationary density  $\mu(\cdot,\cdot)$ . Furthermore, for any Borel measurable function  $f(\cdot,\cdot)$ :  $R^n \times \mathcal{M} \to R$  satisfying

$$\sum_{k \in \mathcal{M}} \int_{\mathbb{R}^n} |f(X,k)| \mu(X,k) \, dz < \infty,$$

the following holds:

$$P\left(\lim_{t\to\infty}\frac{1}{t}\int_0^t f(X(s),r(s))\,ds=\sum_{k\in\mathcal{M}}\int_{R^n}f(X,k)\mu(X,k)\,dz\right)=1.$$

# 3. Dynamic Analysis of the System

3.1. The Existence and Uniqueness of the Positive Solution

**Theorem 1.** For any given initial value  $(T(0), H(0), R(0), r(0)) \in R_3^+ \times \mathcal{M}$ , the system (2) has a unique global solution, (T(t), H(t), R(t), r(t)), such that

$$P\{(T(t), H(t), R(t), r(t)) \in R_3^+ \times \mathcal{M}, \forall t \ge 0\} = 1.$$

**Proof.** To demonstrate the existence of the solution for the system (2), we first construct an auxiliary impulsive-free system, which serves as a simplified framework to investigate the behaviors of the stochastic tumor–immune dynamics. This auxiliary system is governed by the following stochastic differential equations:

Mathematics **2025**, 13, 928 7 of 29

$$\begin{cases} dx_{1}(t) = \left(a_{1}(r(t))x_{1}\left(1 - \frac{\prod\limits_{0 < nP < t}[1 - \alpha(nP)]x_{1}}{c_{1}(r(t))}\right) - b_{1}(r(t))\prod\limits_{0 < nP < t}[1 + \beta(nP)]x_{1}y_{1}\right)dt + \sigma_{1}(r(t))x_{1}dB_{1}(t), \\ dy_{1}(t) = \left(\gamma(r(t))y_{1}z_{1} - d_{1}(r(t))y_{1} - b_{2}(r(t))\prod\limits_{0 < nP < t}[1 - \alpha(nP)]x_{1}y_{1}\right)dt + \sigma_{2}(r(t))y_{1}dB_{2}(t), \\ dz_{1}(t) = \left(a_{2}(r(t))z_{1}\left(1 - \frac{z_{1}}{c_{2}(r(t))}\right) - \gamma(r(t))\prod\limits_{0 < nP < t}[1 + \beta(nP)]y_{1}z_{1} - d_{2}(r(t))z_{1} + \frac{h(r(t))\prod\limits_{0 < nP < t}[1 - \alpha(nP)]x_{1}z_{1}}{\prod\limits_{0 < nP < t}[1 - \alpha(nP)]x_{1} + g(r(t))}\right)dt \\ + \sigma_{3}(r(t))z_{1}dB_{3}(t), \end{cases}$$

$$(3)$$

The initial conditions for the auxiliary system are specified as  $(x_1(0), y_1(0), z_1(0), r(0)) = (T(0), H(0), R(0), r_0)$ , where all initial values are strictly positive. According to Definition 1, the solution derived from the system (3)

$$(T(t), H(t), R(t), r(t)) = \left( \prod_{0 < nP < t} [1 - \alpha(nP)] x_1(t), \prod_{0 < nP < t} [1 + \beta(nP)] y_1(t), z_1(t), r(t) \right)$$

can be regarded as an equivalent solution to the system (2). The positivity of (T(t), H(t), R(t), r(t)) was established in [29] and will not be restated here. Next, we proceed to prove the uniqueness of the solution to the system (2). For any  $t \in (0, P]$  or  $t \in (nP, (n+1)P], n \in Z^+$ , the system (2) is reduced to the following classical equations:

$$dT(t) = \left(a_{1}(r(t))T(t)\left(1 - \frac{T(t)}{c_{1}(r(t))}\right) - b_{1}(r(t))T(t)H(t)\right)dt + \sigma_{1}(r(t))T(t)dB_{1}(t),$$

$$dH(t) = (\gamma(r(t))H(t)R(t) - d_{1}(r(t))H(t) - b_{2}(r(t))H(t)T(t))dt + \sigma_{2}(r(t))H(t)dB_{2}(t),$$

$$dR(t) = \left(a_{2}(r(t))R(t)\left(1 - \frac{R(t)}{c_{2}(r(t))}\right) - \gamma(r(t))H(t)R(t) - d_{2}(r(t))R(t) + \frac{h(r(t))T(t)R(t)}{T(t) + g(r(t))}\right)dt + \sigma_{3}(r(t))R(t)dB_{3}(t).$$

$$(4)$$

Note that the coefficients of the system (4) satisfy the local Lipschitz condition with linear growth, it follows from Mao's theory [35] that there exists a unique local solution

$$(T(t), H(t), R(t), r(t)) \in \mathbb{R}^3_+ \times \mathcal{M}$$

in the interval  $t \in (0, \tau_e]$ , where  $\tau_e$  denotes the explosion time. To establish the global existence of the solution, it is necessary to demonstrate that  $\tau_e = +\infty$ . Given that the initial values are positive and bounded, there exists a sufficiently large number,  $n_0 > 0$ , such that

$$T(0) \in \left[\frac{1}{n_0}, n_0\right], \quad H(0) \in \left[\frac{1}{n_0}, n_0\right], \quad R(0) \in \left[\frac{1}{n_0}, n_0\right].$$

For any  $n > n_0$ , we define

$$\tau_n = \inf \left\{ t \in [0, \tau_e) : T(t) \notin \left[ \frac{1}{n}, n \right], H(t) \notin \left[ \frac{1}{n}, n \right], R(t) \notin \left[ \frac{1}{n}, n \right] \right\}.$$

It is evident that  $\tau_n$  increases as n increases, and  $\tau_n < \tau_e$ . Let

$$\tau_{\infty} = \lim_{n \to \infty} \tau_n.$$

If so, we can prove

$$\tau_{\infty} \leq \tau_e$$
 a.s.

Mathematics 2025, 13, 928 8 of 29

Next, we will use a proof by contradiction. Suppose that there exist constants T > 0 and  $\varepsilon \in (0,1)$  such that

$$P(\tau_{\infty} \leq T) > \varepsilon$$
.

The inequality above means that with positive probability, the process (T(t), H(t), R(t)) will exit the bounded region  $\left[\frac{1}{n}, n\right]$  before the time T for some n. Consequently, there must exist an integer  $n_1 \geq n_0$  such that for all  $n \geq n_1$ ,

$$P(\tau_n < T) > \varepsilon$$
.

Define a Lyapunov function  $W: \mathbb{R}^3_+ \times \mathcal{M} \to \mathbb{R}_+$  as follows:

$$W(T, H, R) = (T + 1 - \log T) + (H + 1 - \log H) + (R + 1 - \log R).$$

By applying Itô's formula [35], we can obtain the expression for the Lyapunov function as

$$\begin{split} \mathcal{L}[W(T,H,R)] &= \left(1 - \frac{1}{T}\right) \left[a_1(r(t))T\left(1 - \frac{T}{c_1(r(t))}\right) - b_1(r(t))TH\right] + \frac{1}{2}\sigma_1^2(r(t)) \\ &+ \left(1 - \frac{1}{H}\right) [\gamma(r(t))HR - d_1(r(t))H - b_2(r(t))HT] + \frac{1}{2}\sigma_2^2(r(t)) \\ &+ \left(1 - \frac{1}{R}\right) \left[a_2(r(t))R\left(1 - \frac{R}{c_2(r(t))}\right) - \gamma(r(t))HR - d_2(r(t))R + \frac{h(r(t))TR}{T + g(r(t))}\right] + \frac{1}{2}\sigma_3^2(r(t)) \\ &\leq \left(\hat{d}_1 + \hat{d}_2 + \frac{1}{2}\hat{\sigma}_1^2 + \frac{1}{2}\hat{\sigma}_2^2 + \frac{1}{2}\hat{\sigma}_3^2\right) + \left(\hat{a}_1 + \frac{\hat{a}_1}{\check{c}_1} + \hat{b}_2\right)T + \left(\hat{b}_1 + \hat{\gamma}\right)H \\ &+ \left(\hat{a}_2 + \hat{h} + \frac{\hat{a}_2}{\check{c}_2}\right)R \end{split}$$

where  $\hat{x} = max(x(r(t))), \check{x} = min(x(r(t)))$ . Let

$$A = \hat{d}_1 + \hat{d}_2 + \frac{1}{2}\hat{\sigma}_1^2 + \frac{1}{2}\hat{\sigma}_2^2 + \frac{1}{2}\hat{\sigma}_3^2 \quad B = 2\max\left\{\hat{a}_1 + \frac{\hat{a}_1}{\check{c}_1} + \hat{b}_2, \hat{b}_1 + \hat{\gamma}, \hat{a}_2 + \hat{h} + \frac{\hat{a}_2}{\check{c}_2}\right\},$$

the above expression can be rewritten as

$$\mathcal{L}[W(T,H,R)] \le A + BW(T,H,R) \tag{5}$$

Consequently, integrating both sides of the inequality (5) from 0 to  $\tau_n \wedge T$  and taking the expectation yields

$$\mathbb{E}\Big[W\Big(T(\tau_{n} \wedge T), H(\tau_{n} \wedge T), R(\tau_{n} \wedge T)\Big)\Big]$$

$$\leq W(T(0), H(0), R(0)) + AT + B\mathbb{E}\Big[\int_{0}^{\tau_{n} \wedge T} W(T(t), H(t), R(t))dt\Big]$$

$$= W(T(0), H(0), R(0)) + AT + B\mathbb{E}\Big[\int_{0}^{T} I_{[0,\tau_{n}]}(t)W(T(t), H(t), R(t))dt\Big]$$

$$\leq W(T(0), H(0), R(0)) + AT + B\int_{0}^{T} \mathbb{E}\Big[W\Big(T(\tau_{n} \wedge T), H(\tau_{n} \wedge T), R(\tau_{n} \wedge T)\Big)\Big]dt$$

$$= W(T(0), H(0), R(0)) + AT + B\int_{0}^{T} \mathbb{E}\Big[W\Big(T(\tau_{n} \wedge T), H(\tau_{n} \wedge T), R(\tau_{n} \wedge T)\Big)\Big]dt.$$

Mathematics 2025, 13, 928 9 of 29

In which  $I_A(\cdot)$  represents the indicator function of the set A, and  $\tau_n \wedge T = \min(\tau_n, T)$ . Using Gronwall's inequality [35], we derive

$$\mathbb{E}[W(T(\tau_n \wedge T), H(\tau_n \wedge T), R(\tau_n \wedge T))] \leq (W(T(0), H(0), R(0)) + AT)e^{BT}.$$

For all  $n \ge n_1$ , we have  $P(\Omega_n) \ge \varepsilon$ , where  $\Omega_n = \{\tau_n \le T\}$ . Consequently, for any  $\omega \in \Omega_n$ , at least one of  $T(\tau_n, \omega)$ ,  $H(\tau_n, \omega)$ , or  $R(\tau_n, \omega)$  equals n or 1/n. Thus,

$$W(T(\tau_n,\omega),H(\tau_n,\omega),R(\tau_n,\omega)) \geq (n-1-\ln n) \wedge \left(\frac{1}{n}-1-\ln n\right).$$

Letting  $n \to \infty$  leads to a contradiction:

$$\infty > (W(T(0), H(0), R(0)) + AT)e^{BT} > \infty.$$

Therefore, we conclude that  $\tau_{\infty} = \infty$ , which implies that  $\tau_e = \infty$ . Hence, the solution to the system (2) is globally unique and positive.  $\square$ 

The auxiliary system (3) provides an essential foundation for analyzing the existence and properties of the solutions to the original impulsive stochastic system (2). By examining the behavior of this simplified model, insights into the persistence and extinction of cell populations under various biological and environmental conditions can be obtained.

3.2. Extinction and Non-Persistence in the Mean

**Theorem 2.** For the system (2), the following conclusions hold:

- (1) Extinction:
  - If  $\Gamma_1 < 0$ , the helper T-cells will eventually go extinct.
  - If  $\Gamma_2 + \hat{\gamma} \frac{\hat{c}_2}{d\hat{\gamma}} \Gamma_1$ , the hunting T-cells will eventually go extinct.
  - If  $\Gamma_3 < 0$ , the tumor cells will eventually go extinct.
- (2) Non-persistence in the mean:
  - If  $\Gamma_1 = 0$ , the helper T-cells are non-persistent in the mean.
  - If  $\Gamma_3 = 0$ , both the hunting T-cells and the tumor cells are non-persistent in the mean.

Here,

$$\begin{split} \Gamma_1 &= \sum_{i \in \mathcal{M}} \pi_i \bigg[ a_2(i) - d_2(i) - \frac{1}{2} \sigma_3^2(i) + h(i) \bigg], \\ \Gamma_2 &= \lim_{t \to \infty} \sup \frac{1}{t} \sum_{0 < nP < t} \ln[1 + \beta(nP)] - \sum_{i \in \mathcal{M}} \pi_i \bigg[ d_1(i) + \frac{1}{2} \sigma_1^2(i) \bigg], \\ \Gamma_3 &= \lim_{t \to \infty} \sup \frac{1}{t} \sum_{0 < nP < t} \ln[1 - \alpha(nP)] + \sum_{i \in \mathcal{M}} \pi_i \bigg[ a_1(i) - \frac{1}{2} \sigma_1^2(i) \bigg]. \end{split}$$

**Proof.** We will proceed with the analysis based on

$$(T(t), H(t), R(t), r(t)) = \left( \prod_{0 \le nP \le t} [1 - \alpha(nP)] x_1(t), \prod_{0 \le nP \le t} [1 + \beta(nP)] y_1(t), z_1(t), r(t) \right).$$

By taking the logarithm of both sides of the system (3) and utilizing the Itô formula [35], we obtain

Mathematics **2025**, 13, 928

$$d \ln x_{1}(t) = \left(a_{1}(r(t)) \left(1 - \frac{\prod\limits_{0 < nP < t} [1 - \alpha(nP)]x_{1}}{c_{1}(r(t))}\right) - b_{1}(r(t)) \prod\limits_{0 < nP < t} [1 + \beta(nP)]y_{1} - \frac{1}{2}\sigma_{1}^{2}(r(t))\right) dt + \sigma_{1}(r(t))dB_{1}(t)$$
(6)
$$= \left(a_{1}(r(t)) \left(1 - \frac{T(t)}{c_{1}(r(t))}\right) - b_{1}(r(t))H(t) - \frac{1}{2}\sigma_{1}^{2}(r(t))\right) dt + \sigma_{1}(r(t))dB_{1}(t),$$
(7)

$$d\ln y_1(t) = \left(\gamma z_1(r(t)) - d_1(r(t)) - b_2(r(t)) \prod_{0 < nP < t} [1 - \alpha(nP)] x_1 - \frac{1}{2}\sigma_2^2(r(t))\right) dt + \sigma_2(r(t)) dB_2(t)$$
(8)

$$= \left(\gamma(r(t))R(t) - d_1(r(t)) - b_2(r(t))T(t) - \frac{1}{2}\sigma_2^2(r(t))\right)dt + \sigma_2(r(t))dB_2(t), \tag{9}$$

$$d\ln z_1(t) = \left(a_2(r(t))\left(1 - \frac{z_1(t)}{c_2(r(t))}\right) - \gamma(r(t))H(t) - d_2(r(t)) + \frac{h(r(t))T(t)}{T(t) + g(r(t))} - \frac{1}{2}\sigma_3^2(r(t))\right)dt + \sigma_3(r(t))dB_3(t). \tag{10}$$

Integrating both sides from 0 to t, the above equations can be rewritten as

$$\ln x_1(t) = \ln x_1(0) + \int_0^t \left(a_1(r(s)) - \frac{1}{2}\sigma_1^2(r(s))\right) dt - \int_0^t \frac{a_1(r(s))}{c_1(r(s))} T(s) \, dt - \int_0^t b_1(r(s)) H(s) \, dt + \int_0^t \sigma_1(r(s)) \, dB_1(t), \quad (11)$$

$$\ln y_1(t) = \ln y_1(0) - \int_0^t \left( d_1(r(s)) + \frac{1}{2}\sigma_2^2(r(s)) \right) dt + \int_0^t \gamma(r(s))R(s) dt - \int_0^t b_2(r(s))T(s) dt + \int_0^t \sigma_2(r(s)) dB_2(t),$$

$$\ln z_{1}(t) = \ln z_{1}(0) + \int_{0}^{t} \left( a_{2}(r(s)) - d_{2}(r(s)) - \frac{1}{2}\sigma_{3}^{2}(r(s)) \right) dt - \int_{0}^{t} \frac{a_{2}(r(s))}{c_{2}(r(s))} z_{1}(s) dt - \int_{0}^{t} \gamma(r(s))H(s) dt + \int_{0}^{t} \frac{h(r(s))T(s)}{T(s) + g(r(s))} dt + \int_{0}^{t} \sigma_{3}(r(s)) dB_{3}(t). \tag{12}$$

As follows,

$$\frac{1}{t} \ln \frac{T(t)}{T(0)} = \frac{1}{t} \sum_{0 < nP < t} \ln[1 - \alpha(nP)] + \ln x_1(t) - \ln x_1(0) 
= \frac{1}{t} \sum_{0 < nP < t} \ln[1 - \alpha(nP)] + \frac{1}{t} \int_0^t \left( a_1(r(s)) - \frac{1}{2}\sigma_1^2(r(s)) \right) dt - \frac{1}{t} \int_0^t \frac{a_1(r(s))}{c_1(r(s))} T(s) dt 
- \frac{1}{t} \int_0^t b_1(r(s)) H(s) dt + \frac{L_1(t)}{t},$$
(13)

$$\frac{1}{t} \ln \frac{H(t)}{H(0)} = \frac{1}{t} \sum_{0 < nP < t} \ln[1 + \beta(nP)] + \ln y_1(t) - \ln y_1(0) 
= \frac{1}{t} \sum_{0 < nP < t} \ln[1 + \beta(nP)] - \frac{1}{t} \int_0^t \left( d_1(r(s)) + \frac{1}{2}\sigma_2^2(r(s)) \right) dt + d\frac{1}{t} \int_0^t \gamma(r(s))R(s) dt 
- \frac{1}{t} \int_0^t b_2(r(s))T(s) dt + \frac{L_2(t)}{t},$$
(14)

$$\frac{1}{t} \ln \frac{R(t)}{R(0)} = \ln z_1(t) - \ln z_1(0) 
= \frac{1}{t} \int_0^t \left( a_2(r(s)) - d_2(r(s)) - \frac{1}{2} \sigma_3^2(r(s)) \right) dt - \frac{1}{t} \int_0^t \frac{a_2(r(s))}{c_2(r(s))} R(s) dt 
- \frac{1}{t} \int_0^t \gamma(r(s)) H(s) dt + \frac{1}{t} \int_0^t \frac{h(r(s)) T(s)}{T(s) + g(r(s))} dt + \frac{L_3(t)}{t}.$$
(15)

Mathematics 2025, 13, 928 11 of 29

where  $L_i(t) = \int_0^t \sigma_i(r(t)) dB_i(s)$  (i = 1, 2, 3) is a real-valued continuous local martingale. Its quadratic variation is given by  $\langle L_i(t), L_i(t) \rangle = \int_0^t \sigma_i^2(r(s)) ds$ . Making use of the strong law of large numbers for local martingales [35], we obtain

$$\lim_{t \to +\infty} \frac{L_i(t)}{t} = 0.(a.s.)$$

# (1) Analysis of the Dynamics of the Helper T-Cells R(t)

**Case of**  $\Gamma_1$  < 0: By considering the upper limit of Equation (15) and given the condition

$$\Gamma_1 = \sum_{i \in \mathcal{M}} \pi_i \left[ a_2(i) - d_2(i) - \frac{1}{2} \sigma_3^2(i) + h(i) \right] < 0,$$

it is concluded that

$$\lim_{t\to\infty}\sup\frac{\ln R(t)}{t}\leq\Gamma_1<0,$$

Which implies that

$$\lim_{t\to\infty}R(t)=0.$$

Hence, according to Definition 2, the helper T-cells will eventually become extinct.

Case of  $\Gamma_1 = 0$ : Let  $\bar{\epsilon} > 0$  be an arbitrarily small constant. Assume that there exists a time  $t_1 > 0$  such that for all  $t \ge t_1$ , the following inequalities hold:

$$\frac{1}{t}\ln z_1(0) \leq \bar{\epsilon} \quad \text{and} \quad \frac{1}{t}\int_0^t \frac{h(r(s))T(s)}{T(s) + g(r(s))} dt \leq h(r(t)) + \frac{\bar{\epsilon}}{2}.$$

By using the expression of Equation (12), we obtain

$$\begin{split} \ln R(t) &= \ln z_1(t) \leq \ln z_1(0) + \int_0^t \left[ a_2(r(s)) - d_2(r(s)) - \frac{1}{2}\sigma_3^2(r(s)) \right] dt - \int_0^t \frac{a_2(r(s))}{c_2(r(s))} z_1(s) dt - \int_0^t \gamma(r(s)) H(s) dt \\ &+ \int_0^t \frac{h(r(s))T(s)}{T(s) + g(r(s))} dt + \frac{L_3(t)}{t} \\ &\leq \sum_{i \in \mathcal{M}} \pi_i \bigg( a_2(i) - d_2(i) - \frac{1}{2}\sigma_3^2(i) + h(i) + \bar{\epsilon} \bigg) t - \frac{\check{a_2}}{\hat{c_2}} \int_0^t z_1(s) ds + \sigma_3 B_3(t). \end{split}$$

Thus we have

$$\ln R(t) \leq (\Gamma_1 + \bar{\epsilon})t - \frac{\check{a_2}}{\hat{c_2}} \int_0^t z_1(s)ds + \sigma_3 B_3(t).$$

Based on Lemma 1, we derive

$$\langle R(t) \rangle^* \le \frac{\Gamma_1 + \bar{\epsilon}}{\frac{\check{a_2}}{\hat{c_2}}}.$$
 (16)

Since  $R(t) \ge 0$ , it follows that

$$\langle R(t) \rangle^* = 0.$$

# (2) Analysis of the Dynamics of the Hunting T-Cells H(t)

**Case of**  $\Gamma_2 + \hat{\gamma} \frac{\hat{c_2}}{\check{a_2}} \Gamma_1 < 0$ : Considering Equation (16) and the arbitrarily small constant  $\bar{\epsilon} > 0$  in Equation (16), we deduce that

$$\langle R(t) \rangle^* \leq \frac{\hat{c_2}\Gamma_1}{\check{a_2}}.$$

Mathematics **2025**, 13, 928

Taking the upper limit of Equation (14) yields

$$\lim_{t\to\infty}\sup\frac{\ln H(t)}{t}\leq \Gamma_2+\hat{\gamma}\frac{\hat{c_2}}{\check{a_2}}\Gamma_1<0.$$

This implies that

$$\lim_{t\to\infty}H(t)=0,$$

which indicates that the hunting T-cells will eventually go extinct.

**Case of**  $\Gamma_3 = 0$ : Reviewing Equation (13), we have

$$\frac{1}{t} \int_{0}^{t} b_{1}(r(s))H(s) dt = -\frac{1}{t} \ln \frac{T(t)}{T(0)} + \frac{1}{t} \sum_{0 < nP < t} [1 - \alpha(nP)] + \frac{1}{t} \int_{0}^{t} \left[ a_{1}(r(s)) - \frac{1}{2}\sigma_{1}^{2}(r(s)) \right] dt - \frac{1}{t} \int_{0}^{t} \frac{a_{1}(r(s))T(s)}{c_{1}(r(s))} dt + \frac{L_{1}(t)}{t}.$$
(17)

By evaluating the upper limit of Equation (17), we obtain

$$\hat{b}_1 \langle H(t) \rangle^* \leq \Gamma_3 + \bar{\varepsilon},$$

where  $\bar{\epsilon}$  is a sufficiently small constant. If  $\Gamma_3 = 0$ , it follows that

$$\langle H(t) \rangle^* \leq 0.$$

Consider that  $H(t) \geq 0$ , we conclude that

$$\langle H(t) \rangle^* = 0$$
,

which indicates that the hunting T-cells are non-persistent in the mean sense.

(3) Analysis of the Dynamics of the Tumor Cells T(t)

**Case of**  $\Gamma_3$  < 0: Consider the following equation:

$$\frac{1}{t} \ln \frac{T(t)}{T(0)} = \frac{1}{t} \sum_{0 < nP < t} [1 - \alpha(nP)] + \frac{1}{t} \int_0^t \left[ a_1(r(t)) - \frac{1}{2} \sigma_1^2(r(t)) \right] dt - \frac{1}{t} \int_0^t \frac{a_1(r(t))}{c_1(r(t))} T(t) dt - \frac{1}{t} \int_0^t b_1(r(t)) H(t) dt + \frac{1}{t} \int_0^t \sigma_1(r(t)) dB_1(t).$$

Taking the upper limit of the above equation as  $t \to \infty$ , we obtain

$$\lim_{t\to\infty}\sup\frac{1}{t}\ln T(t)\leq\Gamma_3<0.$$

Which implies that

$$\lim_{t\to\infty}T(t)=0,$$

which indicates that the tumor cell population vanishes as  $t \to \infty$ .

**Case of**  $\Gamma_3 = 0$ : Let  $\varepsilon_1 > 0$  be an arbitrarily small constant. Then, there exists a time  $t_2 > 0$  such that for all  $t \ge t_2$ , the following conditions hold:

$$\frac{x_1(0)}{t} \le \varepsilon_1/2, \quad \frac{1}{t} \sum_{0 < nP < t} \left[ 1 - \alpha(nP) \right] \le \lim_{t \to \infty} \sup \frac{1}{t} \sum_{0 < nP < t} \left[ 1 - \alpha(nP) \right] + \varepsilon_1/2.$$

Mathematics 2025, 13, 928 13 of 29

Substitute the above equation into Equation (11), we obtain

$$\ln T(t) \le \left(\frac{x_1(0)}{t} + \frac{1}{t} \sum_{0 < nP < t} \left[1 - \alpha(nP)\right] + \sum_{i \in \mathcal{M}} \pi_i \left[a_1(i) - \frac{1}{2}\sigma_1^2(i)\right]\right) t$$
$$- \int_0^t \frac{a_1(r(s))}{c_1(r(s))} T(s) dt - \int_0^t b_1(r(s)) H(s) dt + \int_0^t \sigma_1(r(s)) dB_1(t).$$

Simplify the above further, we have

$$\ln T(t) \leq (\Gamma_3 + \varepsilon_1)t - \frac{\check{a_1}}{\hat{c_1}} \int_0^t T(s) dt + \sigma_1(r(t))B_1(t).$$

Applying Lemma 1, it follows that

$$\langle T(t) \rangle^* \leq \frac{\Gamma_3 + \varepsilon_1}{\check{a_1}/\hat{c_1}}.$$

As For  $\Gamma_3 = 0$ , which reduces to

$$\langle T(t) \rangle^* \leq 0$$
,

Meanwhile  $T(t) \ge 0$ , therefore

$$\langle T(t) \rangle^* = 0.$$

The result above indicates that the tumor cell population is non-persistent in the mean sense.  $\Box$ 

3.3. Weak Persistence

**Theorem 3.** Assuming that  $\Gamma_3 > 0$  and  $\Gamma_2 + \hat{\gamma} \frac{\hat{c_2}}{\check{a_2}} \Gamma_1 < 0$ , the tumor cells will exhibit weak persistence.

Proof. We proceed by contradiction. Assume that

$$\frac{1}{t} \ln \frac{T(t)}{T(0)} \le 0$$

is false, i.e., T(t) > 0, which leads to

$$\langle T(t) \rangle^* > 0.$$

Review Equation (13), we have

$$\frac{1}{t} \ln \frac{T(t)}{T(0)} = \frac{1}{t} \sum_{0 < nP < t} [1 - \alpha(nP)] + \frac{1}{t} \int_0^t \left[ a_1(r(s)) - \frac{1}{2} \sigma_1^2(r(s)) \right] dt 
- \frac{1}{t} \int_0^t \frac{a_1(r(s))}{c_1(r(s))} T(s) dt - \frac{1}{t} \int_0^t b_1(r(s)) H(s) dt + \frac{L_1(t)}{t} \le 0.$$
(18)

Take the upper limit on both sides of Equation (18), we obtain

$$\frac{\hat{a_1}}{\check{c_1}}T(t)\rangle^* + \hat{b_1}\langle H(t)\rangle^* \ge \Gamma_3 > 0. \tag{19}$$

As follows, we continue to the proof by contradiction. Suppose that

$$\langle T(t) \rangle^* \leq 0$$
,

Mathematics 2025, 13, 928 14 of 29

which implies that

$$\langle T(t) \rangle^* = 0.$$

Therefore, for any  $\omega \in \{\langle T(t,\omega)\rangle^* = 0\}$ , we obtain from Equation (19)

$$\langle H(t,\omega)\rangle^* > 0.$$

Furthermore, take the upper limit of Equation (14), we obtain

$$\lim_{t\to\infty}\frac{1}{t}\ln\frac{H(t)}{H(0)}\leq \Gamma_2+\hat{\gamma}\langle R(t)\rangle^*\leq \Gamma_2+\hat{\gamma}\frac{\hat{c_2}}{\check{a_2}}\Gamma_1<0.$$

The result above implies that

$$\langle H(t,\omega)\rangle^* = 0$$
,

which contradicts the fact that  $\langle H(t,\omega)\rangle^*>0$ . Therefore, the assumption that  $\langle T(t)\rangle^*\leq 0$  is false, and it must be true that

$$\langle T(t) \rangle^* > 0.$$

Thus we conclude that the tumor cells exhibit weakly persistence.  $\Box$ 

#### 3.4. Stationary Distribution

Theorem 4. If

$$\lambda = \sum_{k=1}^{m} \pi_k \Lambda_k = \sum_{i \in \mathcal{M}} \pi_i \left[ a_1(i) + a_2(i) - d_1(i) - d_2(i) - \frac{1}{2} \sigma_1^2(i) - \frac{1}{2} \sigma_2^2(i) - \frac{1}{2} \sigma_3^2(i) \right] < 0,$$

then for any given initial condition,

$$(T(0), H(0), R(0), r(0)) \in R^3_+ \times \mathcal{M}$$

the system (2) admits a unique ergodic stationary distribution.

**Proof.** Using Itô's formula [35], the system (3) becomes

$$d\ln x_1(t) = \left(a_1(r(t))\left(1 - \frac{\prod\limits_{0 < nP < t} [1 - \alpha(nP)]x_1}{c_1(r(t))}\right) - b_1(r(t))\prod\limits_{0 < nP < t} [1 + \beta(nP)]y_1 - \frac{1}{2}\sigma_1^2(r(t))\right)dt + \sigma_1(r(t))dB_1(t),$$
(20)

$$d\ln y_1(t) = \left(\gamma z_1(r(t)) - d_1(r(t)) - b_2(r(t)) \prod_{0 < nP < t} [1 - \alpha(nP)] x_1 - \frac{1}{2}\sigma_2^2(r(t))\right) dt + \sigma_2(r(t)) dB_2(t), \tag{21}$$

$$d\ln z_1(t) = \left(a_2(r(t))\left(1 - \frac{z_1(t)}{c_2(r(t))}\right) - \gamma(r(t))H(t) - d_2(r(t)) + \frac{h(r(t))T(t)}{T(t) + g(r(t))} - \frac{1}{2}\sigma_3^2(r(t))\right)dt + \sigma_3(r(t))dB_3(t). \tag{22}$$

The system (3) can be rewritten as follows by defining  $x(t) = \ln(x_1(t)), y(t) = \ln(y_1(t)), z(t) = \ln(z_1(t)),$ 

Mathematics **2025**, 13, 928 15 of 29

$$dx(t) = \left(a_{1}(r(t))\left(1 - \frac{\prod\limits_{0 < nP < t} [1 - \alpha(nP)]e^{x}}{c_{1}(r(t))}\right) - b_{1}(r(t))\prod\limits_{0 < nP < t} [1 + \beta(nP)]e^{y} - \frac{1}{2}\sigma_{1}^{2}(r(t))\right)dt + \sigma_{1}(r(t))dB_{1}(t),$$

$$dy(t) = \left(\gamma(r(t))e^{z} - d_{1}(r(t)) - b_{2}(r(t))\prod\limits_{0 < nP < t} [1 - \alpha(nP)]e^{x} - \frac{1}{2}\sigma_{2}^{2}(r(t))\right)dt + \sigma_{2}(r(t))dB_{2}(t),$$

$$dz(t) = \left(a_{2}(r(t))\left(1 - \frac{e^{z}}{c_{2}(r(t))}\right) - \gamma(r(t))\prod\limits_{0 < nP < t} [1 + \beta(nP)]e^{y} - d_{2}(r(t)) + \frac{h(r(t))\prod\limits_{0 < nP < t} [1 - \alpha(nP)]e^{x}}{\prod\limits_{0 < nP < t} [1 - \alpha(nP)]e^{x} + h(r(t))} + \frac{1}{2}\sigma_{3}^{2}(r(t))\right)dt + \sigma_{3}(r(t))dB_{3}(t).$$

$$(23)$$

On the basis of the proof in [34], it can be concluded that the ergodicity of the system (3) is equivalent to the ergodicity of the system (23). Therefore, we only need to verify that the system (23) satisfies the conditions in Lemma 2. We assume that  $\theta_{ij} > 0$  for all  $i \neq j$ , which ensures that condition (1) in Lemma 2 is satisfied. Let  $H(X,k) = \operatorname{diag}(\sigma_1(k),\sigma_2(k),\sigma_3(k))$  for  $k \in \mathcal{M}$ ; then,

$$D(X,k) = H(X,k)H^{T}(X,k) = \operatorname{diag}(\sigma_{1}^{2}(k), \sigma_{2}^{2}(k), \sigma_{3}^{2}(k)),$$

which is positive definite. This indicates that condition (2) in Lemma 2 is satisfied. We now proceed to verify condition (3) in Lemma 2.

Let the function  $\phi(x, y, z)$  be defined as

$$\phi(x,y,z) = \frac{1}{1+\theta}(e^x + e^y + e^z)^{1+\theta} + M(-x - y - z), \quad \theta \in (0,1),$$

where M is a constant. It is clear that  $\phi(x,y,z)$  has a minimum value, denoted as  $\phi(x_0,y_0,z_0)$ . Then we have

$$\phi(x,y,z) - \phi(x_0,y_0,z_0) > 0.$$

Define a non-negative function  $V: \mathbb{R}^3 \times \mathcal{M} \to \mathbb{R}^+ \cup \{0\}$  as

$$V(x, y, z, k) = \phi(x, y, z) - \phi(x_0, y_0, z_0) + M(\vartheta_k + |\vartheta|),$$

where

$$V_1(x,y,z) = \frac{1}{1+\theta} (e^x + e^y + e^z)^{1+\theta},$$
  
 $V_2(x,y,z) = M(-x-y-z),$   
 $V_3(k) = (\vartheta_k + |\vartheta|),$ 

and  $\vartheta = (\vartheta_1, \vartheta_2, \dots, \vartheta_m)^T$ , with

$$|\vartheta| = \sqrt{\vartheta_1^2 + \vartheta_2^2 + \dots + \vartheta_m^2}.$$

The term  $\vartheta_k$  (for  $k \in \mathcal{M}$ ) will be defined below. The expression  $|\vartheta|$  ensures the non-negativity of  $(\vartheta_k + |\vartheta|)$ . Therefore, V(x, y, z, k) is non-negative.

By applying Itô's formula [35], we derive the following expression:

Mathematics 2025, 13, 928 16 of 29

$$\begin{split} \mathcal{L}V_1 &= (e^x + e^y + e^z)^\theta \left[ a_1(k) \left( 1 - \frac{\prod\limits_{0 < nP < t} [1 - \alpha(nP)] e^x}{c_1(k)} \right) e^x - b_1(k) \prod\limits_{0 < nP < t} [1 + \beta(nP)] e^{x+y} \right. \\ &+ \gamma(k) e^{y+z} - d_1(k) e^y - b_2(k) \prod\limits_{0 < nP < t} [1 - \alpha(nP)] e^{x+y} \\ &+ a_2(k) \left( 1 - \frac{e^z}{c_2(k)} \right) e^z - \gamma(k) \prod\limits_{0 < nP < t} [1 + \beta(nP)] e^{y+z} - d_2(k) e^z \\ &+ \frac{h(k) \prod\limits_{0 < nP < t} [1 - \alpha(nP)] e^{x+z}}{\prod\limits_{0 < nP < t} [1 - \alpha(nP)] e^x + g(k)} \right] + \frac{\theta}{2} (e^x + e^y + e^z)^{\theta - 1} \left( \sigma_1^2(k) e^{2x} + \sigma_2^2(k) e^{2y} + \sigma_3^2(k) e^{2z} \right) \\ &\leq 3^\theta (e^{\theta x} + e^{\theta y} + e^{\theta z}) \left[ a_1(k) e^x + \gamma(r(t)) e^{y+z} + a_2(k) e^z + h(k) e^z \right] \\ &- \frac{a_1(k) \prod\limits_{0 < nP < t} [1 - \alpha(nP)] e^{(2+\theta)x}}{c_1(k)} - d_1(k) e^{(1+\theta)y} - \frac{a_2(k) e^{(2+\theta)z}}{c_2(k)} - d_2(k) e^{(1+\theta)z} \\ &+ \frac{\theta}{2} \left( \sigma_1^2(k) e^{(1+\theta)x} + \sigma_2^2(k) e^{(1+\theta)y} + \sigma_3^2(k) e^{(1+\theta)z} \right) \\ &\leq - \frac{a_1(k) \prod\limits_{0 < nP < t} [1 - \alpha(nP)]}{2c_1(k)} e^{(2+\theta)x} - \frac{d_1(k)}{2} e^{(1+\theta)y} - \frac{a_2(k)}{2c_2(k)} e^{(2+\theta)z} \\ &+ 3^\theta (a_2(k) + h(k)) e^{\theta x + z} + 3^\theta a_1(k) e^{x + \theta y} + 3^\theta (a_2(k) + h(k)) e^{\theta y + z} + 3^\theta a_1(k) e^{x + \theta z} + I'. \end{split}$$

where

$$\begin{split} I' &= -\frac{a_1(k) \prod\limits_{0 < nP < t} [1 - \alpha(nP)]}{2c_1(k)} e^{(2+\theta)x} - \frac{d_1(k)}{2} e^{(1+\theta)y} - \frac{a_2(k)}{2c_2(k)} e^{(2+\theta)z} - d_2(k) e^{(1+\theta)z} \\ &+ 3^{\theta} a_1(k) e^{(1+\theta)x} + 3^{\theta} \gamma(k) e^{\theta x + y + z} + 3^{\theta} \gamma(k) e^{(1+\theta)y + z} + 3^{\theta} \gamma(k) e^{y + (1+\theta)z} \\ &+ 3^{\theta} (a_2(k) + h(k)) e^{(\theta+1)z} + \frac{\theta}{2} \sigma_1^2(k) e^{(1+\theta)x} + \frac{\theta}{2} \sigma_2^2(k) e^{(1+\theta)y} + \frac{\theta}{2} \sigma_3^2(k) e^{(1+\theta)z}. \end{split}$$

Similarly, the computation of  $\mathcal{L}(-x-y-z)$  yields

$$\begin{split} \mathcal{L}(-x-y-z) &= -\left[a_1(k)\left(1 - \frac{\prod\limits_{0 < nP < t}[1 - \alpha(nP)]e^x}{c_1(k)}\right) - b_1(k)\prod\limits_{0 < nP < t}[1 + \beta(nP)]e^y - \frac{1}{2}\sigma_1^2(k)\right] \\ &- \left[\gamma(k)e^z - d_1(k) - b_2(k)\prod\limits_{0 < nP < t}[1 - \alpha(nP)]e^x - \frac{1}{2}\sigma_2^2(k)\right] \\ &- \left[a_2(k)\left(1 - \frac{e^z}{c_2(k)}\right) - \gamma(k)\prod\limits_{0 < nP < t}[1 + \beta(nP)]e^y - d_2(k) \right. \\ &+ \frac{h(k)\prod\limits_{0 < nP < t}[1 - \alpha(nP)]e^x}{\prod\limits_{0 < nP < t}[1 - \alpha(nP)]e^x + h(k)} + \frac{1}{2}\sigma_3^2(k)\right] \\ &\leq \left[\frac{a_1(k)\prod\limits_{0 < nP < t}[1 - \alpha(nP)]}{c_1(k)} + b_2(k)\prod\limits_{0 < nP < t}[1 - \alpha(nP)]\right]e^x \\ &+ \left[b_1(k)\prod\limits_{0 < nP < t}[1 + \beta(nP)] + \gamma(k)\prod\limits_{0 < nP < t}[1 + \beta(nP)]\right]e^y + \frac{a_2(k)}{c_2(k)}e^z \\ &- \left[a_1(k) + a_2(k) - d_1(k) - d_2(k) - \frac{1}{2}\sigma_1^2(k) - \frac{1}{2}\sigma_2^2(k) - \frac{1}{2}\sigma_3^2(k)\right]. \end{split}$$

Mathematics **2025**, 13, 928 17 of 29

For any  $k \in \mathcal{M}$ , we have

$$\mathcal{L}V_3(k) = \sum_{l \in \mathcal{M}} \theta_{kl} \vartheta_l.$$

Define the vector  $\Lambda = (\Lambda_1, \Lambda_2, \dots, \Lambda_m)^T$ , where

$$\Lambda_k = a_1(k) + a_2(k) - d_1(k) - d_2(k) - \frac{1}{2}\sigma_1^2(k) - \frac{1}{2}\sigma_2^2(k) - \frac{1}{2}\sigma_3^2(k).$$

Observe that  $\Gamma$  is irreducible, there exists the vector  $\vartheta = (\vartheta_1, \vartheta_2, \dots, \vartheta_m)^T$ , satisfying the following system:

$$\Gamma artheta = -\sum_{k=1}^m \pi_k \Lambda_k egin{pmatrix} 1 \ dots \ 1 \end{pmatrix} + \Lambda.$$

Hence the *k*-th element of the vector  $\Gamma \vartheta - \Lambda$  is

$$\sum_{l \in M} \theta_{kl} \vartheta_l - \left(\alpha_1(k) + \alpha_2(k) - \delta_1(k) - \delta_2(k) - \frac{1}{2} \xi_1^2(k) - \frac{1}{2} \xi_2^2(k) - \frac{1}{2} \xi_3^2(k)\right) = -\sum_{k=1}^m \pi_k \Lambda_k = -\lambda.$$

Correspondingly, we have

$$\begin{split} \mathcal{L}V(x,y,z,k) &\leq -M\lambda - \frac{a_1(k) \prod\limits_{0 < nP < t} [1 - \alpha(nP)]}{2c_1(r(t))} e^{(2+\theta)x} - \frac{d_1(r(t))}{2} e^{(1+\theta)y} - \frac{a_2(r(t))}{2c_2(r(t))} e^{(2+\theta)z} \\ &+ 3^{\theta}(a_2 + h)e^{\theta x + z} + 3^{\theta}a_1e^{x + \theta y} + 3^{\theta}(a_2 + k)e^{\theta y + z} + 3^{\theta}a_1e^{x + \theta z} + I, \end{split}$$

where

$$I = I' + M \left[ \frac{a_1(k) \prod_{0 < nP < t} (1 - \alpha(nP))}{c_1(k)} + b_2(k) \prod_{0 < nP < t} (1 - \alpha(nP)) \right] e^x$$

$$+ \left( b_1(k) \prod_{0 < nP < t} (1 + \beta(nP)) + \gamma(k) \prod_{0 < nP < t} (1 + \beta(nP)) \right) e^y + \frac{a_2(k)}{c_2(k)} e^z.$$

For any sufficiently small  $0 < \epsilon < 1$ , we define the open set  $\Omega$  with a compact closure as

$$\Omega = \left\{ (x, y, z) : |x| < \ln(\epsilon^{-1}), |y| < \ln(\epsilon^{-1}), |z| < \ln(\epsilon^{-1}), (x, y, z) \in \mathbb{R}^3 \right\}.$$

The next step, we prove that

$$\mathcal{L}V(x,y,z,k) < -1$$
 holds on  $\Omega^{\mathcal{C}} \times \mathcal{M}$ .

In domain  $\Omega^{\mathbb{C}} \times \mathcal{M}$ , we select a M such that

$$M > \frac{2}{\lambda} \max \left\{ 2, \sup_{(x,y,z) \in R^3} \left( I + 3^{\theta} (\hat{a}_2 + \hat{h}) e^{\theta y + z} \right), \sup_{(x,y,z) \in R^3} \left( 3^{\theta} (\hat{a}_2 + \hat{h}) e^{\theta x + z} + 3^{\theta} \hat{a}_1 e^{x + \theta z} + I \right), \sup_{(x,y,z) \in R^3} \left( 3^{\theta} \hat{a}_1 e^{x + \theta y} + I \right) \right\}. \tag{24}$$

A sufficiently small  $\epsilon$  can be chosen such that

$$\epsilon^{\theta} < \frac{\check{d}_1}{2 \cdot 3^{\theta} \max\{\hat{a}_1, \hat{a}_2 + \hat{h}\}},\tag{25}$$

$$\epsilon^{\theta} < \frac{\check{a}_2}{2 \cdot 3^{\theta} \hat{k}_2 (\hat{a}_1 + \hat{a}_2 + \hat{h})},\tag{26}$$

Mathematics 2025, 13, 928 18 of 29

$$\epsilon^{\theta} < \frac{M\lambda}{8 \cdot 3^{\theta} (\hat{a}_1 + \hat{a}_2 + \hat{h})},\tag{27}$$

$$\epsilon^{\theta} < \frac{\check{a}_1 \prod\limits_{0 < nP < t} [1 - a(nP)]}{3^{\theta} \hat{k}_1 (\hat{a}_1 + \hat{a}_2 + \hat{h})},\tag{28}$$

$$-M\lambda - \frac{\hat{a}_1 \prod\limits_{0 < nP < t} [1 - \alpha(nP)]}{2\check{c}_1 \epsilon^{2+\theta}} + I_1 < -1, \tag{29}$$

$$-M\lambda - \frac{\hat{d}_1}{2\epsilon^{1+\theta}} + I_2 < -1,\tag{30}$$

$$-M\lambda - \frac{\hat{a}_2}{2\check{c}_2\epsilon^{2+\theta}} + I_3 < -1. \tag{31}$$

Define the following six sets:

$$\begin{split} &\Omega^1_{\epsilon} = \Big\{ (x,y,z) \in R^3 : -\infty \leq x \leq \ln(\epsilon) \Big\}, \qquad \Omega^4_{\epsilon} = \Big\{ (x,y,z) \in R^3 : x \geq \ln(\epsilon^{-1}) \Big\}, \\ &\Omega^2_{\epsilon} = \Big\{ (x,y,z) \in R^3 : -\infty \leq y \leq \ln(\epsilon) \Big\}, \qquad \Omega^5_{\epsilon} = \Big\{ (x,y,z) \in R^3 : y \geq \ln(\epsilon^{-1}) \Big\}, \\ &\Omega^3_{\epsilon} = \Big\{ (x,y,z) \in R^3 : -\infty \leq z \leq \ln(\epsilon) \Big\}, \qquad \Omega^6_{\epsilon} = \Big\{ (x,y,z) \in R^3 : z \geq \ln(\epsilon^{-1}) \Big\}. \end{split}$$

If so, we have

$$\Omega^C = \Omega^1_\varepsilon \cup \Omega^2_\varepsilon \cup \Omega^3_\varepsilon \cup \Omega^4_\varepsilon \cup \Omega^5_\varepsilon \cup \Omega^6_\varepsilon.$$

So what we should prove next is that

$$\mathcal{L}V(x,y,z,k) < -1$$

holds in  $\Omega_{\epsilon}^i \times \mathcal{M}$  for i = 1, ..., 6.

**Case 1:** In  $\Omega^1_{\epsilon} \times \mathcal{M}$ , we have the following inequalities:

$$e^{\theta x + z} \le \epsilon^{\theta} e^z \le \epsilon^{\theta} (1 + e^{(2 + \theta)z}), \quad e^{x + \theta y} \le \epsilon^{\theta} e^{\theta y} \le \epsilon^{\theta} (1 + e^{(1 + \theta)y}), \quad e^{x + \theta z} \le \epsilon^{\theta} e^{\theta z} \le \epsilon^{\theta} (1 + e^{(2 + \theta)z}).$$

Therefore, we can express the following inequality for  $\mathcal{L}V(x,y,z,k)$ :

$$\begin{split} \mathcal{L}V(x,y,z,k) & \leq -M\lambda - \frac{a_1(k) \prod\limits_{0 < nP < t} [1 - \alpha(nP)]}{2c_1(k)} e^{(2+\theta)x} - \frac{d_1(k)}{2} e^{(1+\theta)y} - \frac{a_2(k)}{2c_2(k)} e^{(2+\theta)z} \\ & + 3^{\theta}(a_2(k) + h(k)) e^{\theta x + z} + 3^{\theta}a_1(k) e^{x + \theta y} + 3^{\theta}(a_2(k) + h(k)) e^{\theta y + z} + 3^{\theta}a_1(k) e^{x + \theta z} + I \\ & \leq -\frac{M\lambda}{4} - \frac{\hat{a}_1 \prod\limits_{0 < nP < t} [1 - \alpha(nP)]}{2\check{c}_1} e^{(2+\theta)x} + \left( -\frac{\hat{d}_1}{2} + 3^{\theta}\check{a}_1\epsilon^{\theta} \right) e^{(1+\theta)y} \\ & + \left( -\frac{\hat{a}_2}{2\check{c}_2} + 3^{\theta}(\check{a}_1 + \check{a}_2(k) + \check{h})\epsilon^{\theta} \right) e^{(2+\theta)z} + \left( -\frac{M\lambda}{4} + 3^{\theta}(\check{a}_2 + \check{h})\epsilon^{\theta} + 2\check{a}_13^{\theta}\epsilon^{\theta} \right) \\ & + \left( -\frac{M\lambda}{2} + I + 3^{\theta}(\check{a}_2 + \check{h})e^{\theta y + z} \right). \end{split}$$

Mathematics 2025, 13, 928 19 of 29

From Equations (24)–(27), we obtain

$$\mathcal{L}V(x,y,z,k) < -1.$$

**Case 2:** In  $\Omega_{\epsilon}^2 \times \mathcal{M}$ , we have the following inequalities:

$$e^{x+\theta y} \le \epsilon^{\theta} (1 + e^{(2+\theta)x}), \quad e^{\theta y+z} \le \epsilon^{\theta} (1 + e^{(2+\theta)z}).$$

Therefore, we can express the following inequality for  $\mathcal{L}V(x,y,z,k)$ :

$$\begin{split} LV(x,y,z,k) &\leq -\frac{M\lambda}{4} - \left(\frac{\hat{a}_1 \prod\limits_{0 < nP < t} [1 - \alpha(nP)]}{2\check{c}_1} + 3^{\theta} \check{a}_1 \epsilon^{\theta}\right) e^{(2+\theta)x} - \frac{\hat{d}_1}{2} e^{(1+\theta)y} \\ &- \left(\frac{\hat{a}_2}{2\check{c}_2} + 3^{\theta} (\check{a}_2 + \check{h}) \epsilon^{\theta}\right) e^{(2+\theta)z} + \left(-\frac{M\lambda}{4} + 3^{\theta} \check{a}_1 \epsilon^{\theta} + 3^{\theta} (\check{a}_2 + \check{h}) \epsilon^{\theta}\right) \\ &+ \left(-\frac{M\lambda}{2} + 3^{\theta} (\check{a}_2 + \check{h}) e^{\theta x + z} + 3^{\theta} \check{a}_1 e^{x + \theta z} + I\right) \end{split}$$

Based on Equations (24), (26) and (27), we obtain

$$\mathcal{L}V(x,y,z,k) \leq -1.$$

**Case 3:** In  $\Omega^3_{\epsilon} \times \mathcal{M}$ , we have the following inequalities:

$$e^{\theta x+z} \le \epsilon^{\theta} (1+e^{(2+\theta)x}), \quad e^{\theta y+z} \le \epsilon^{\theta} (1+e^{(1+\theta)y}), \quad e^{x+\theta z} \le \epsilon^{\theta} (1+e^{(2+\theta)x}).$$

In this way, we can express the following inequality for  $\mathcal{L}V(x,y,z,k)$ :

$$\begin{split} \mathcal{L}V(x,y,z,k) &\leq -\frac{M\lambda}{4} + \left(-\frac{\hat{a}_1 \prod\limits_{0 < nP < t} [1 - \alpha(nP)]}{2\check{c}_1} + 3^{\theta} (\check{a}_2 + \check{h}) \epsilon^{\theta} + 3^{\theta} \check{a}_1 \epsilon^{\theta}\right) e^{(2+\theta)x} \\ &+ \left(3^{\theta} (\check{a}_2 + \check{h}) \epsilon^{\theta} - \frac{\hat{a}_1}{2}\right) e^{(1+\theta)y} - \frac{\hat{a}_2}{2\check{c}_2} e^{(2+\theta)z} \\ &+ \left(-\frac{M\lambda}{4} + 2(\check{a}_2 + \check{h}) 3^{\theta} \epsilon^{\theta} + 3^{\theta} \check{a}_1 \epsilon^{\theta}\right) + \left(-\frac{M\lambda}{2} + 3\theta \check{a}_1 e^{x+\theta y} + I\right). \end{split}$$

Based on Equations (24), (25), (27), and (28), we obtain

$$\mathcal{L}V(x, y, z, k) \leq -1.$$

**Case 4:** In  $\Omega_{\epsilon}^4 \times \mathcal{M}$ , we have the following inequality for  $\mathcal{L}V(x,y,z,k)$ :

Mathematics 2025, 13, 928 20 of 29

$$\begin{split} \mathcal{L}V(x,y,z,k) & \leq -M\lambda - \frac{a_1(k) \prod\limits_{0 < nP < t} [1 - \alpha(nP)]}{2c_1(k)} e^{(2+\theta)x} \\ & + \left[ -\frac{d_1(k)}{2} e^{(1+\theta)y} - \frac{a_2(k)}{2c_2(k)} e^{(2+\theta)z} + 3\theta(a_2(k) + h(k)) e^{\theta x + z} \right. \\ & + 3^{\theta}a_1(k)e^{x+\theta y} + 3^{\theta}(a_2(k) + h(k))e^{\theta y + z} + 3^{\theta}a_1(k)e^{x+\theta z} + I \right] \\ & \leq -M\lambda - \frac{\hat{a}_1 \prod\limits_{0 < nP < t} [1 - \alpha(nP)]}{2\check{c}_1\epsilon^{2+\theta}} + I_1. \end{split}$$

In which

$$I_1 = -\frac{2d_1(k)}{2}e^{(1+\theta)y} - \frac{2c_2(k)a_2(k)}{2}e^{(2+\theta)z} + 3^{\theta}(a_2(k) + h(k))e^{\theta x + z} + 3^{\theta}a_1e^{x + \theta y} + 3^{\theta}(a_2 + h)e^{\theta y + z} + 3^{\theta}a_1e^{x + \theta z} + I.$$

Because of Equation (29), we obtain

$$\mathcal{L}V(x,y,z,k) \leq -1.$$

**Case 5:** In  $\Omega^5_{\epsilon} \times \mathcal{M}$ , we have

$$\begin{split} \mathcal{L}V(x,y,z,k) &\leq -M\lambda - \frac{d_1(k)}{2}e^{(1+\theta)y} + \left[ -\frac{a_1(k)\prod\limits_{0 < nP < t} [1-\alpha(nP)]}{2c_1(k)}e^{(2+\theta)x} \right. \\ & \left. -\frac{a_2(k)}{2c_2(k)}e^{(2+\theta)z} + 3^{\theta}(a_2(k) + h(k))e^{\theta x + z} + 3^{\theta}a_1(k)e^{x + \theta y} + 3^{\theta}(a_2(k) + h(k))e^{\theta y + z} + 3^{\theta}a_1(k)e^{x + \theta z} + I \right] \\ & \leq -M\lambda - \frac{\hat{d}_1}{2\epsilon^{1+\theta}} + I_2, \end{split}$$

in which

$$I_{2} = -\frac{a_{1}(k) \prod\limits_{0 < nP < t} [1 - \alpha(nP)]}{2c_{1}(k)} e^{(2+\theta)x} - \frac{a_{2}(k)}{2c_{2}(k)} e^{(2+\theta)z} + 3^{\theta}(a_{2}(k) + h(k))e^{\theta x + z} + 3^{\theta}a_{1}(k)e^{x + \theta y} + 3^{\theta}(a_{2}(k) + h(k))e^{\theta y + z} + 3^{\theta}a_{1}(k)e^{x + \theta z} + I.$$

From Equation (30), we obtain

$$\mathcal{L}V(x,y,z,k) \leq -1.$$

**Case 6:** In  $\Omega_{\epsilon}^6 \times \mathcal{M}$ , we have

$$\begin{split} \mathcal{L}V(x,y,z,k) & \leq -M\lambda - \frac{a_2(k)}{2c_2(k)}e^{(2+\theta)z} + \left[ -\frac{a_1(k)\prod\limits_{0 < nP < t}[1-\alpha(nP)]}{2c_1(k)}e^{(2+\theta)x} \right. \\ & \left. -\frac{d_1(k)}{2}e^{(1+\theta)y} + 3^{\theta}(a_2(k) + h(k))e^{\theta x + z} + 3^{\theta}a_1e^{x + \theta y} + 3^{\theta}(a_2(k) + h(k))e^{\theta y + z} + 3^{\theta}a_1(k)e^{x + \theta z} + I \right] \\ & \leq -M\lambda - \frac{\hat{a}_2}{2\check{c}_2\epsilon^{2+\theta}} + I_3, \end{split}$$

where

Mathematics 2025, 13, 928 21 of 29

$$I_{3} = -\frac{a_{1}(k) \prod\limits_{0 < nP < t} [1 - \alpha(nP)]}{2c_{1}(k)} e^{(2+\theta)x} - \frac{d_{1}(k)}{2} e^{(1+\theta)y} + 3^{\theta}(a_{2} + h)e^{\theta x + z} + 3^{\theta}a_{1}e^{x + \theta y} + 3^{\theta}(a_{2} + h)e^{\theta y + z} + 3^{\theta}a_{1}e^{x + \theta z} + I.$$

By way of Equation (31), we obtain

$$\mathcal{L}V(x, y, z, k) \leq -1.$$

As a conclusion, we have

$$\mathcal{L}V(x,y,z,k) \le -1$$
 for  $(x,y,z,k) \in R_3^+ \times \mathcal{M}$ .

Correspondingly, the solution of the system (2) is positively recurrent and has a unique stationary distribution.  $\Box$ 

# 4. Numerical Simulations

The Milstein high-order method [36] is an efficient and accurate numerical method for solving stochastic differential equations (SDEs). It can transform continuous SDEs into a series of discrete approximations by discretizing the time step, thereby achieving numerical solutions to the original equations. The strengths of the Milstein high-order method lies not only in its ability to enhance the solution accuracy by introducing the second-order term into Itô's formula but also in solving various types of SDEs, including linear and nonlinear equations. Particularly, this method is capable to solve SDEs with Markov regime switching. Therefore, we choose to employ this method for the subsequent numerical simulation. The initial conditions are set as

$$T(0) = 5 \times 10^9$$
 (cells),  $H(0) = 4 \times 10^6$  (cells),  $R(0) = 3 \times 10^8$  (cells).

For simplicity, it is assumed that the Markov chain r(t) takes values in the state space  $\mathcal{M} = \{1,2\}$ . If the Markov chain has the generator matrix

$$\Xi = \begin{bmatrix} -3 & 3 \\ 7 & -7 \end{bmatrix},$$

the stationary distribution  $\pi=(\pi_1,\pi_2)$  can be determined by solving the linear system of equations

$$\pi\Xi=0,\quad \sum_{k=1}^2\pi_k=1,$$

yielding  $\pi = (0.7, 0.3)$ .

Figure 2 illustrates the switching behavior of the Markov chain r(t) in the state space  $\mathcal{M}=\{1,2\}$ . Each state in the model corresponds to a specific combination of biological conditions (such as a high metabolic/low-oxygen state), and the switching frequency is determined by the statistical law of long-term observational data. This steady-state probability-based switching mechanism essentially synchronizes invisible microenvironmental fluctuations with a regulated rhythm of therapeutic intervention, enabling discrete clinical decision-making processes to effectively track continuous biological dynamics.

Mathematics **2025**, 13, 928

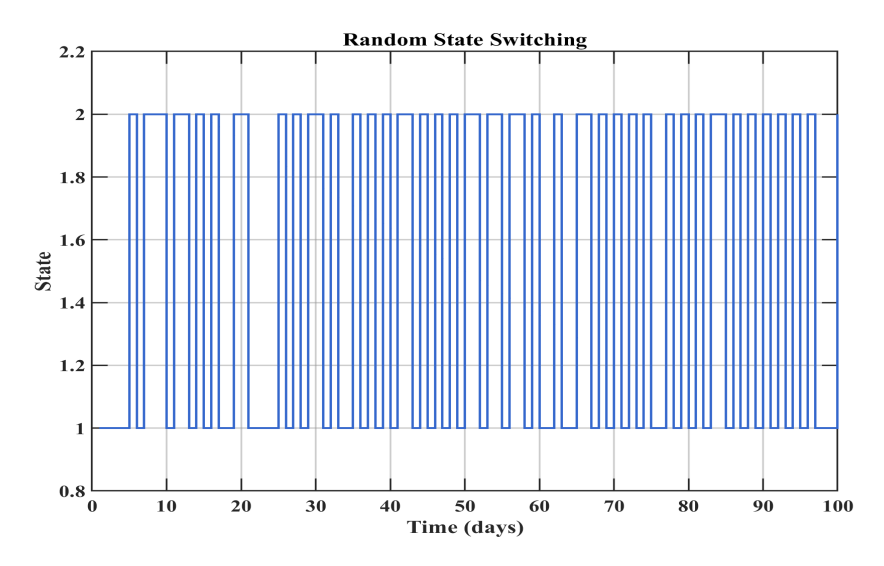


**Figure 2.** Switching behavior of Markov chain r(t) in state space  $\mathcal{M} = \{1,2\}$ .

Next, we numerically verify the extinction of tumor cells, hunting T-cells, and helper T-cells. The timescale for the extinction dynamics spans several dozen to several hundred days, depending on the model parameters and biological conditions. This range aligns with empirical observations, where tumor elimination through treatment or the immune response typically occurs over weeks to months. Rapid clearance is observed in highly effective treatment scenarios, whereas slower extinction may result from gradual immune-mediated suppression or a partial therapeutic response. The mathematical model captures these dynamics by incorporating key factors such as the tumor growth rate, immune response strength, and stochastic fluctuations, ensuring biological realism in the predicted extinction timescale. The parameter values [26] are given as follows:

$$\begin{split} a_1(1) &= a_1(2) = 0.18/\text{day}, \quad a_2(1) = a_2(2) = 0.0245/\text{day}, \\ b_1(1) &= b_1(2) = 1.101 \times 10^{-7}/\text{cells/day}, \quad b_2(1) = b_2(2) = 3.422 \times 10^{-10}/\text{cells/day}, \\ d_1(1) &= d_1(2) = 0.0412/\text{day}, \quad d_2(1) = d_2(2) = 0.002/\text{day}, \\ \frac{1}{c_1(1)} &= \frac{1}{c_1(2)} = 2 \times 10^{-9}/\text{cells}, \quad \frac{1}{c_2(1)} = \frac{1}{c_2(2)} = 1 \times 10^{-9}/\text{cells}, \\ \gamma(1) &= \gamma(2) = 6.2 \times 10^{-9}/\text{cells/day}, \quad h(1) = h(2) = 0.1245/\text{day}, \\ g(1) &= g(2) = 2.019 \times 10^7 \text{ cells}. \end{split}$$

As examples, the following intensities of white noise with different scenarios are considered:

$$\begin{split} (\mathcal{H}_1): \quad & \sigma_1(1) = \sigma_1(2) = 1; \, \sigma_2(1) = \sigma_2(2) = 1; \, \sigma_3(1) = 0.6, \, \sigma_3(2) = 0.5, \\ (\mathcal{H}_2): \quad & \sigma_1(1) = \sigma_1(2) = 1; \, \sigma_2(1) = 0.3, \, \sigma_2(2) = 0.1; \, \sigma_3(1) = 0.6, \, \sigma_3(2) = 0.4, \\ (\mathcal{H}_3): \quad & \sigma_1(1) = 0.65, \, \sigma_1(2) = 0.6; \, \sigma_2(1) = \sigma_2(2) = 2; \, \sigma_3(1) = \sigma_3(2) = 2. \end{split}$$

Through calculation, the following results are obtained for  $\mathcal{H}_1$ ,  $\mathcal{H}_2$ , and  $\mathcal{H}_3$ :

$$\begin{split} &\Gamma_1 = \sum_{i \in M} \pi_i \left[ a_2(i) - d_2(i) - \frac{1}{2} \sigma_3^2(i) + h(i) \right] = -0.0165 < 0, \\ &\Gamma_2 + \hat{\gamma} \frac{\hat{c_2}}{\tilde{a_2}} \Gamma_1 = -0.8329 < 0, \\ &\Gamma_3 = \frac{1}{t} \sum_{0 \le nP \le t} \ln[1 - \alpha(nP)] + \sum_{i \in M} \pi_i \left[ a_1(i) - \frac{1}{2} \sigma_1^2(i) \right] = -0.0229 < 0. \end{split}$$

Mathematics 2025, 13, 928 23 of 29

According to Theorem 2, tumor cells, hunting T-cells, and helper T-cells will eventually go extinct. These results are validated in Figure 3a–c.

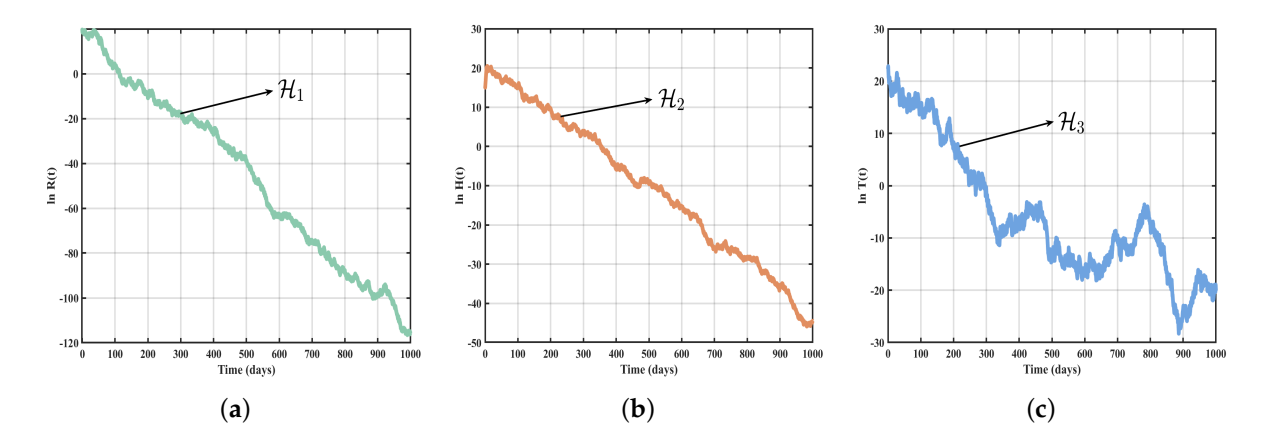


**Figure 3.** (a) Extinction dynamics of helper T–Cells; (b) Extinction dynamics of hunting T–Cells; (c) Extinction dynamics of tumor cells.  $(\mathcal{H}_1): \sigma_1(1) = \sigma_1(2) = 1; \sigma_2(1) = \sigma_2(2) = 1; \sigma_3(1) = 0.6; \sigma_3(2) = 0.5.$   $(\mathcal{H}_2): \sigma_1(1) = \sigma_1(2) = 1; \sigma_2(1) = 0.3; \sigma_2(2) = 0.1; \sigma_3(1) = 0.6; \sigma_3(2) = 0.4.$   $(\mathcal{H}_3): \sigma_1(1) = 0.65; \sigma_1(2) = 0.6; \sigma_2(1) = \sigma_2(2) = 2; \sigma_3(1) = \sigma_3(2) = 2.$ 

Keeping other parameters unchanged, we set

$$\sigma_1(1) = 0.5$$
;  $\sigma_1(2) = 0.2$ ;  $\sigma_2(1) = \sigma_2(2) = 2$ ;  $\sigma_3(1) = \sigma_3(2) = 2$ .

Figure 4a,b show the numerical simulation results of the system (2) under the stationary distributions  $\pi=(0,1)$  and  $\pi=(1,0)$ , respectively. To comprehensively analyze how switching probabilities influence the average population size of tumor cells, we extend the timescale as much as possible. A longer timescale allows us to observe the long-term trends and stabilization effects. These results are consistent with the analytical conclusions of Theorem 3. Furthermore, we observe that under weak persistence, when the noise intensity  $\xi_1$  increases from 0.2 to 0.5, the number of tumor cells significantly decreases. This phenomenon indicates that higher noise intensity effectively suppresses tumor cell growth, validating the critical role of noise interference in the control of tumor dynamics.

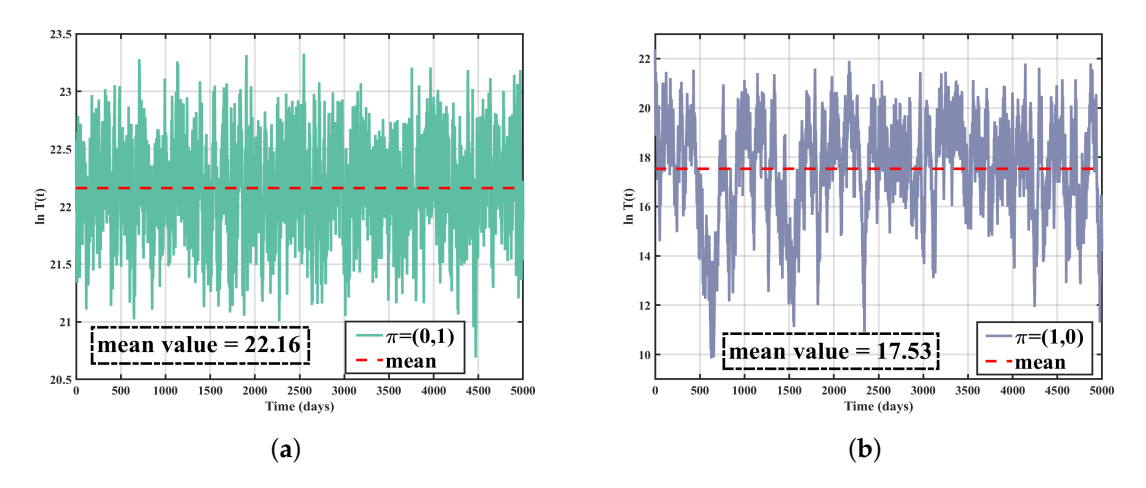


**Figure 4.** Numerical analysis of tumor cell dynamics under steady-state distributions. (a):  $\pi = (0,1)$ ; (b):  $\pi = (1,0)$ .

Next, we investigate the impact of random switching probabilities between different states on tumor regression under the condition of tumor persistence, as shown in Figure 5. The results indicate that when the probability of the system being exposed to

Mathematics 2025, 13, 928 24 of 29

high-noise-intensity states increases, the average number of tumor cells decreases significantly. This suggests that increasing the switching probability to high-noise-intensity states can effectively suppress tumor cells.

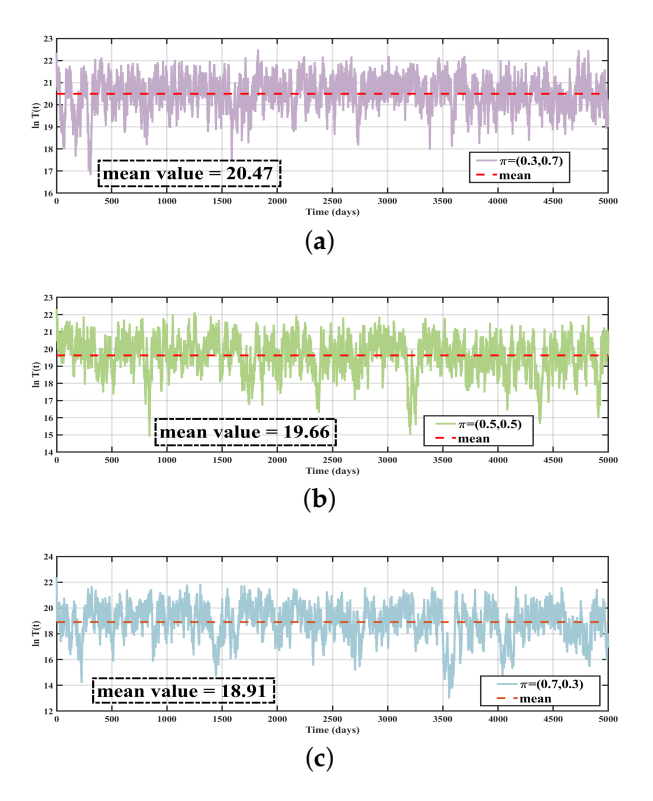


**Figure 5.** Effects of different switching probabilities on tumor dynamics under persistent states. (a):  $\pi = (0.3, 0.7)$ ; (b):  $\pi = (0.5, 0.5)$ ; and (c):  $\pi = (0.7, 0.3)$ .

# 4.1. Impact of Noise Intensity

By keeping the parameters  $\sigma_1(2)=0.5$ ,  $\sigma_2(1)=2$ ,  $\sigma_2(2)=1.5$ ,  $\sigma_3(1)=2$ , and  $\sigma_3(2)=1.5$  unchanged, the stationary probability distribution is set as  $\pi=(0.7,0.3)$ .

Figure 6 explores the long-term dynamics of tumor cells under different values of  $\sigma_1(1)$ . Specifically,  $\sigma_1(1)$  is chosen as 0.3, 0.5, and 0.7, respectively. Comparing the subplots in Figure 6a–c, it can be observed that as  $\sigma_1(1)$  increases from 0.3 to 0.5, the tumor cell clearance effect gradually strengthens. Furthermore, when  $\sigma_1(1)$  increases from 0.5 to 0.7, the persistence of tumor cells transitions to extinction. These results demonstrate that environmental disturbances, by increasing noise intensity, can significantly suppress tumor cell growth, with stronger noise showing more pronounced inhibitory effects. This study suggests that appropriately adjusting the intensity of random disturbances is an effective approach to controlling the dynamics of tumor cells, providing new insights and theoretical support for optimizing tumor treatment strategies.

Mathematics **2025**, 13, 928 25 of 29

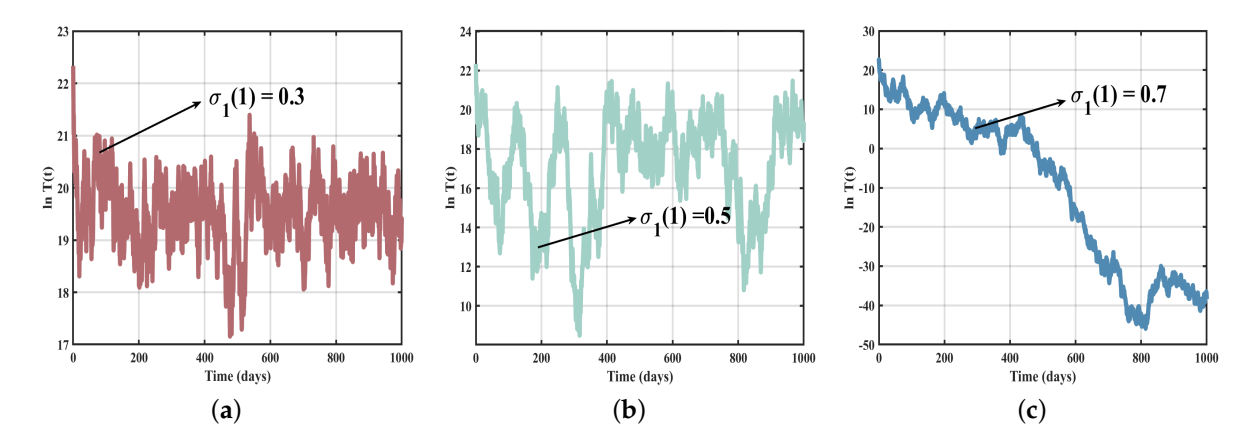


**Figure 6.** Influence of increasing noise intensity  $\sigma_1(1)$  on tumor cell dynamics under steady—state distribution  $\pi = (0.7, 0.3)$ . (a):  $\sigma_1(1) = 0.3$ ; (b):  $\sigma_1(1) = 0.5$ ; and (c):  $\sigma_1(1) = 0.7$ .

### 4.2. Impact of State Switching

To analyze the impact of state switching on tumor cell dynamics, we set the parameters  $\sigma_1(1)=0.7$ ;  $\sigma_1(2)=0.5$ ;  $\sigma_2(1)=\sigma_2(2)=2$ ; and  $\sigma_3(1)=\sigma_3(2)=2$ . In the subsequent numerical simulations, we study the system's behavior under different stationary distributions,  $\pi$ , of the Markov chain. The varying values of  $\pi$  represent different relative dwell times of the system in the two states during the switching process.

Figure 7 illustrates the tumor cell behavior when the system remains entirely in state 2 or state 1, corresponding to persistence and extinction, respectively. When the switching probability between state 1 and state 2 changes (see Figure 8), it is observed that as the dwell time in state 1 (high noise intensity) increases, the number of tumor cells gradually decreases, exhibiting a transition from persistence to extinction. These results demonstrate that extending the exposure time of the system to a high-noise-intensity state can significantly suppress tumor cell growth. This further highlights the potential role of stochastic state switching in controlling tumor dynamics.

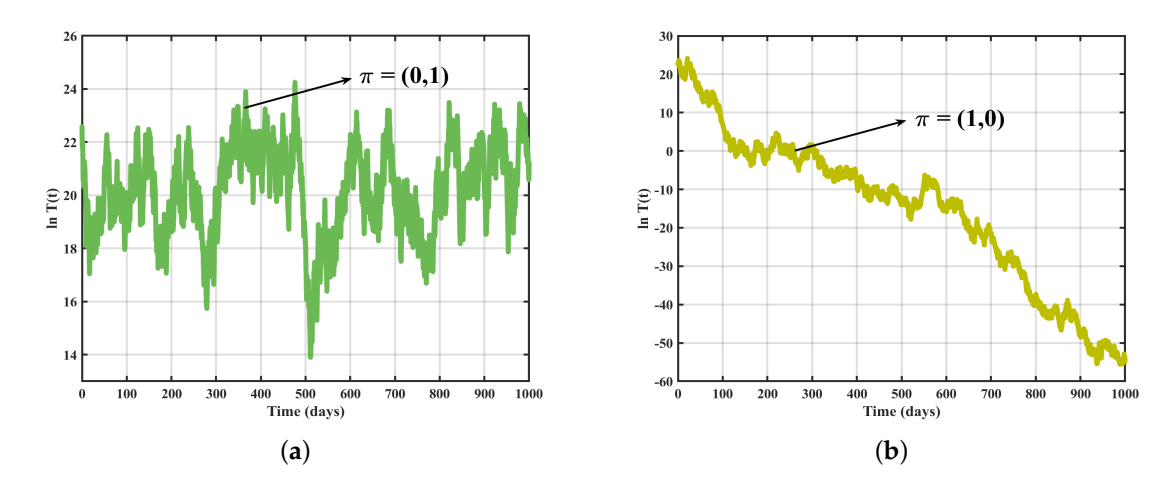


**Figure 7.** Tumor Cell dynamics: a comparison between state 1 and state 2. (a)  $(\pi = (1,0))$ ; (b)  $(\pi = (0,1))$ .

Mathematics 2025, 13, 928 26 of 29

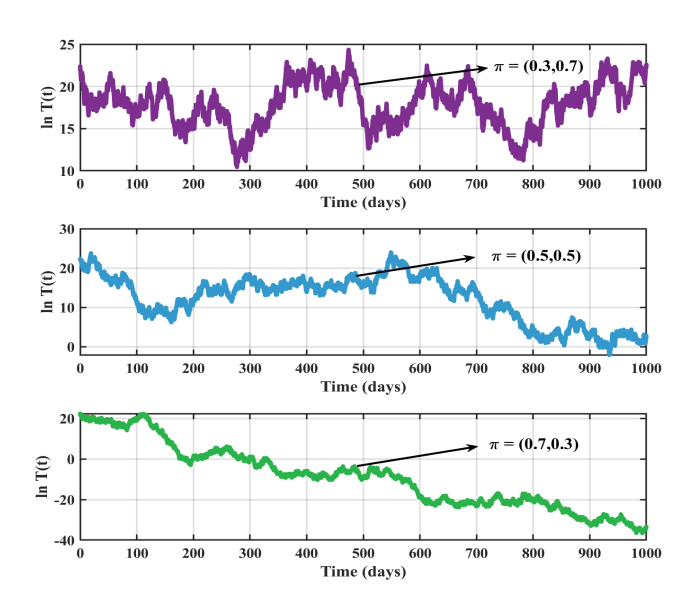
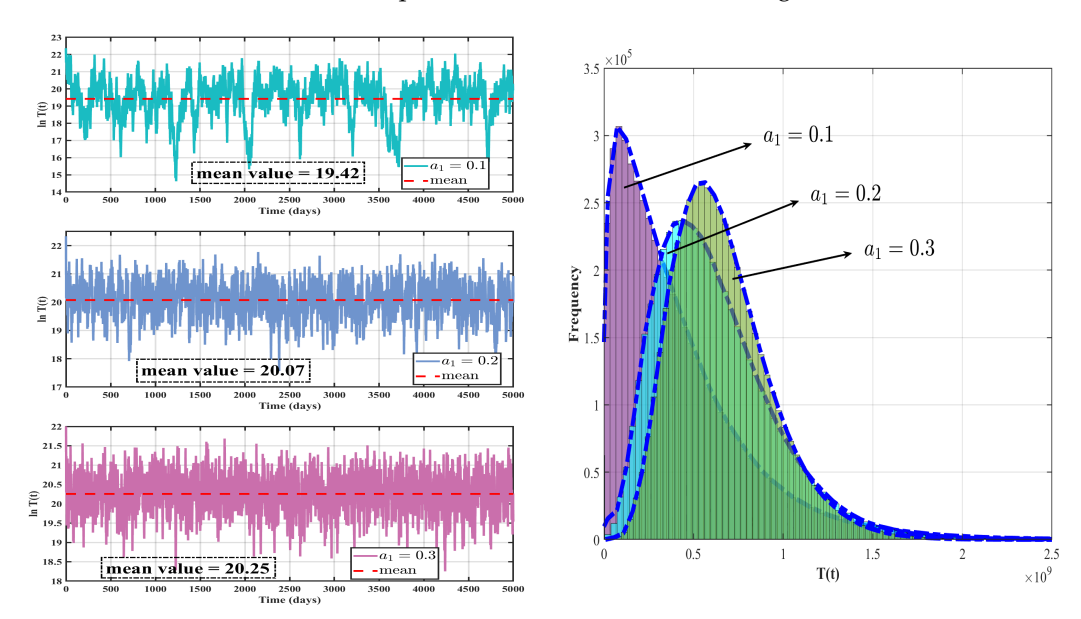


Figure 8. Effect of switching probabilities on tumor dynamics.

## 4.3. Impact of $a_1$

Finally, we analyze the effect of different growth factors,  $a_1$ , on the long-term behavior of tumor cells by adjusting the parameter  $a_1$ . The specific parameter settings for analysis are as follows:  $\sigma_1(1) = 0.2$ ;  $\sigma_1(2) = 0.4$ ;  $\sigma_2(1) = \sigma_2(2) = 1.5$ ;  $\sigma_3(1) = \sigma_3(2) = 1.5$ ; and  $a_1(1) = a_1(2) = 0.1, 0.2, 0.3$ .

As shown in Figure 9, the left panel demonstrates the trends in the average value of tumor cells for different values of  $a_1$ . It can be observed that as  $a_1$  increases, the average value of tumor cells exhibits a gradual upward trend. The right panel of Figure 9 depicts the steady-state distribution corresponding to different values of  $a_1$ . It reveals that as  $a_1$  increases from 0.1 to 0.3, the concentrated range of tumor cell quantity distribution shifts progressively to the right, and the tumor cell count correspondingly increases. These findings reveal the significant influences of the growth factor  $a_1$  on the long-term behavior of tumor cells. An increase in  $a_1$  promotes tumor cell growth, providing theoretical insights for the further development of tumor treatment strategies.



**Figure 9.** Impact of growth factor  $a_1$  on tumor cell dynamics and steady-state distribution.

Mathematics 2025, 13, 928 27 of 29

#### 5. Conclusions

In this study, we establish a stochastic differential equation model based on continuoustime Markov chains to investigate the random dynamics and state-switching phenomena induced by changes in the tumor microenvironment. Our results demonstrate that environmental regime switching plays an essential role in the dynamics of tumor cells. Specifically, we demonstrate the following:

- 1. In the presence of high-intensity white noise, tumor cell growth is significantly suppressed, with the suppression effect further enhanced by prolonged exposure.
- 2. The relevant results of the extinction, persistence, and existence of the stationary distribution in the system address the importance of white noise intensity and exposure duration in influencing tumor dynamics, highlighting their potential as key factors in designing effective tumor control strategies.

Our results show two strategies that can be used in clinical practice. These strategies are based on stochastic modeling. High-intensity noise has been shown to suppress tumors, so we suggest changing traditional chemotherapy methods to include controlled randomness. For example, we could use random dosing intervals (like varying from standard schedules) or change drug concentrations between high and low every 72 hours to mimic helpful environmental changes. Imaging methods should also include assessments of randomness in the microenvironment. This could involve measuring changes in tumor boundaries in regular MRI scans as early warnings of pathological state changes. While the model yielded meaningful insights, it is crucial to note that real-world clinical applications require careful consideration of individual patient conditions, including tumor heterogeneity and potential side effects. Future research should focus on integrating more complex interactions within the tumor microenvironment and validating the theoretical predictions through experimental and clinical studies.

**Author Contributions:** J.Z.: Writing—review and editing, Methodology, Software, Visualization. B.W.: Writing, Data curation, Software, Visualization. W.L.: Supervision, Funding acquisition. D.H.: Writing—review and editing. V.R.: Writing—review and editing. All authors have read and agreed to the published version of the manuscript.

**Funding:** This research was funded by the National Natural Science Foundation of China (Nos. 12272283 and 12172266).

Data Availability Statement: Data will be made available on request.

**Conflicts of Interest:** The authors declare that they have no known competing financial interests or personal relationships that could have appeared to influence the work reported in this paper.

# References

- 1. Guckenberger, M.; Opitz, I.; Dafni, U.; Fontecedro, A.C.; Scherz, A.; Elicin, O.; Addeo, A.; Aerts, J.; Dingemans, A.M.; Hendriks, L.; et al. 1417TiP Immunotherapy, chemotherapy and stereotactic radiotherapy to metastases, followed by definitive surgery or radiotherapy to the primary tumour, in patients with synchronous oligo-metastatic NSCLC: The ETOP CHESS trial. *Ann. Oncol.* 2020, *31*, S895–S896.
- 2. Qu, X.; Zhou, D.; Lu, J.; Qin, D.; Zhou, J.; Liu, H.J. Cancer nanomedicine in preoperative therapeutics: Nanotechnology-enabled neoadjuvant chemotherapy, radiotherapy, immunotherapy, and phototherapy. *Bioact. Mater.* **2023**, *24*, 136–152.
- 3. Groenewold, M.D.; Olthof, C.G.; Bosch, D.J. Anaesthesia after neoadjuvant chemotherapy, immunotherapy or radiotherapy. *BJA Educ.* **2022**, *22*, 12–19.
- Ganesan, P.; Sekaran, S.; Ramasamy, P.; Ganapathy, D. Systematic analysis of chemotherapy, immunotherapy, and combination therapy in Head and Neck Squamous Cell Carcinoma (HNSCC) clinical trials: Focusing on overall survival and progression-free survival outcomes. *Oral Oncol. Rep.* 2024, 12, 100673.

Mathematics **2025**, 13, 928 28 of 29

5. Pang, L.; Shen, L.; Zhao, Z. Mathematical modelling and analysis of the tumor treatment regimens with pulsed immunotherapy and chemotherapy. *Comput. Math. Methods Med.* **2016**, 2016, 6260474.

- 6. Yang, J.; Tang, S.; Cheke, R.A. Modelling pulsed immunotherapy of tumour–immune interaction. *Math. Comput. Simul.* **2015**, 109, 92–112.
- 7. Tang, S.; Li, S.; Tang, B.; Wang, X.; Xiao, Y.; Cheke, R.A. Hormetic and synergistic effects of cancer treatments revealed by modelling combinations of radio-or chemotherapy with immunotherapy. *BMC Cancer* **2023**, 23, 1040.
- 8. Zhao, Z.; Pang, L.; Li, Q. Analysis of a hybrid impulsive tumor-immune model with immunotherapy and chemotherapy. *Chaos Solitons Fractals* **2021**, 144, 110617.
- 9. Rouf, S.; Moore, C.; Saha, D.; Nguyen, D.; Bleile, M.L.; Timmerman, R.; Peng, H.; Jiang, S. PULSAR Effect: Revealing potential synergies in combined radiation therapy and immunotherapy via differential equations. *J. Theor. Biol.* **2025**, *596*, 111974.
- 10. Bashkirtseva, I.; Ryashko, L.; Seoane, J.M.; Sanjuán, M.A. Chaotic transitions in a tumor-immune model under chemotherapy treatment. *Commun. Nonlinear Sci. Numer. Simul.* **2024**, 132, 107946.
- 11. Ngoc, N.T.Y.; Khoa, V.A. An explicit Fourier-Klibanov method for an age-dependent tumor growth model of Gompertz type. *Appl. Numer. Math.* **2024**, *198*, 401–418.
- 12. Khaliq, R.; Iqbal, P.; Bhat, S.A.; Sheergojri, A.R. A fuzzy mathematical model for tumor growth pattern using generalized Hukuhara derivative and its numerical analysis. *Appl. Soft Comput.* **2022**, *118*, 108467.
- 13. Dehingia, K.; Das, P.; Upadhyay, R.K.; Misra, A.K.; Rihan, F.A.; Hosseini, K. Modelling and analysis of delayed tumour–immune system with hunting T-cells. *Math. Comput. Simul.* (*MATCOM*) **2023**, 203, 669–684.
- 14. Wang, J.; Shi, H.; Xu, L.; Zang, L. Hopf bifurcation and chaos of tumor-Lymphatic model with two time delays. *Chaos, Solitons Fractals* **2022**, *157*, 111922.
- 15. Aamer, Z.; Jawad, S.; Batiha, B.; Ali, A.H.; Ghanim, F.; Lupaş, A.A. Evaluation of the Dynamics of Psychological Panic Factor, Glucose Risk and Estrogen Effects on Breast Cancer Model. *Computation* **2024**, *12*, 160.
- 16. Guo, Y.; Yao, T.; Wang, L.; Tan, J. Levy noise-induced transition and stochastic resonance in a tumor growth model. *Appl. Math. Model.* **2021**, *94*, 506–515.
- 17. Hua, M.; Wu, Y. Cross-correlated sine-Wiener noises-induced transitions in a tumor growth system. *Commun. Nonlinear Sci. Numer. Simul.* **2023**, *126*, 107489.
- 18. Li, D.; Xu, W.; Guo, Y.; Xu, Y. Fluctuations induced extinction and stochastic resonance effect in a model of tumor growth with periodic treatment. *Phys. Lett. A* **2011**, *375*, 886–890.
- 19. Lv, H.; He, G.; Cheng, H.; Peng, Y. Stochastic behaviors of an improved Gompertz tumor growth model with coupled two types noise. *Heliyon* **2022**, *8*, e11574.
- 20. Deng, Y.; Liu, M. Analysis of a stochastic tumor-immune model with regime switching and impulsive perturbations. *Appl. Math. Model.* **2020**, *78*, 482–504.
- 21. Yu, X.; Yuan, S.; Zhang, T. Persistence and ergodicity of a stochastic single species model with Allee effect under regime switching. *Commun. Nonlinear Sci. Numer. Simul.* **2018**, *59*, 359–374.
- 22. Chen, X.; Li, X.; Ma, Yuting Yuan, C. The threshold of stochastic tumor-immune model with regime switching. *J. Math. Anal. Appl.* **2023**, 522, 126956.
- 23. Dritschel, H.; Waters, S.; Roller, A.; Byrne, H. A mathematical model of cytotoxic and helper T cell interactions in a tumor microenvironment. *Lett. Biomath.* **2018**, *5*, 1–33.
- 24. Gaach, M. Dynamics of the tumor-immune system competition: The effect of time delay. *Int. J. Appl. Math. Comput. Sci.* **2003**, 13, 395–406.
- 25. Yokoyama, W.M.; Kim, S.; French, A.R. The dynamic life of natural killer cells. Annu. Rev. Immunol. 2004, 22, 405–429.
- 26. Yang, H.; Tan, Y.; Yang, J. Dynamic behavior of stochastic prostate cancer system with comprehensive therapy under regime switching. *Appl. Math. Model.* **2023**, *113*, 398–415.
- 27. Kaur, G.; Ahmad, N. On Study of Immune Response to Tumor Cells in Prey-Predator System. *Int. Sch. Res. Not.* **2014**, 2014, 346597.
- 28. Bingshuo, W.; Li, W.; Zhao, J.; Trišović, N. Longtime evolution and stationary response of a stochastic tumor-immune system with resting T cells. *Math. Biosci. Eng. Spec. Issue Model. Investig. -Predat.-Prey Dyn.* **2024**, 21, 2813–2834.
- 29. Li, W.; Wang, B.; Huang, D.; Rajic, V.; Zhao, J. Dynamical properties of a stochastic tumor–immune model with comprehensive pulsed therapy. *Commun. Nonlinear Sci. Numer. Simul.* **2025**, 140, 108330.
- 30. Wang, L.; Jiang, D.; Feng, T. Threshold dynamics in a stochastic chemostat model under regime switching. *Phys. A Stat. Mech. Its Appl.* **2022**, 599, 127454.
- 31. Zhan, J.; Wei, Y. Dynamical behavior of a stochastic non-autonomous distributed delay heroin epidemic model with regime-switching. *Chaos Solitons Fractals* **2024**, *184*, 115024.
- 32. Zhang, S.; Tan, D. Dynamics of a stochastic predator–prey system in a polluted environment with pulse toxicant input and impulsive perturbations. *Appl. Math. Model.* **2015**, *39*, 6319–6331.

Mathematics **2025**, 13, 928 29 of 29

33. Zhao, Y.; Yuan, S.; Ma, J. Survival and Stationary Distribution Analysis of a Stochastic Competitive Model of Three Species in a Polluted Environment. *Bull. Math. Biol.* **2015**, 77, 1285–1326.

- 34. Liu, H.; Li, X.; Yang, Q. The ergodic property and positive recurrence of a multi-group Lotka–Volterra mutualistic system with regime switching. *Syst. Control. Lett.* **2013**, *62*, 805–810.
- 35. Mao, X.; Yuan, C. Stochastic Differential Equations with Markovian Switching; Imperial College Press: London, UK, 2006.
- Higham.; Desmond, J. An Algorithmic Introduction to Numerical Simulations of Stochastic Differential Equations. SIAM Rev. 2001, 43, 525–546.

**Disclaimer/Publisher's Note:** The statements, opinions and data contained in all publications are solely those of the individual author(s) and contributor(s) and not of MDPI and/or the editor(s). MDPI and/or the editor(s) disclaim responsibility for any injury to people or property resulting from any ideas, methods, instructions or products referred to in the content.